Provisional chapter

High Voltage Pulse Generators Developed in the University of Pau in France for Ultra Wideband Applications

L. Pecastaing, M. Rivaletto, A. Silvestre de Ferron,
B. Cadilhon and R. Pecquois

Additional information is available at the end of the chapter

1. Introduction

The needs in product miniaturization and compact power sources as well as those related to metrology are ever-increasing. In particular, in the field of pulsed sources, the developed sources are now extremely efficient in terms of power per unit volume.

Since 1998, the Electrical Engineering team of the SIAME laboratory of the University of Pau develops various high voltage pulse sources especially dedicated for military applications. Our work consists of improving performance in terms of delivered peak power while keeping the system very small sizes.

This chapter will present various high pulsed power generators developed in the University of Pau in France. These pulse generators are essentially dedicated to ultra wideband (UWB) applications as electromagnetic jammers to disturb or destroy electronics and also UWB radars for electromagnetic detection. The output voltage can reach several hundreds kV with rise-times less than 100ps for example. The corresponding spectrum can extend up to 3GHz. For these works, our main collaborators in France are the DGA, the CEA, XLIM, CISTEME, TECHNIX, ISL or HI PULSE.

This chapter will be focused on:

- Two compact sources based on a Marx generator with their integrated pulse forming line. The main performances of each one are respectively 150kV/200ps/100Hz and 250kV/300ps/350Hz. They are dedicated to electromagnetic jammers.

- A pulse generator dedicated for UWB radar applications. It is very compact and can deliver 25kV/60ps/900Hz pulses.

Their structure, performances, sizes are very different and they will be explained.

2. Generation of high voltage UWB pulses

An electromagnetic radiative source is generally composed of a primary energy storage module, a DC/DC voltage converter, a pulsed power amplifier which may be associated with single-stage pulse sharpening and antenna (Figure 1).

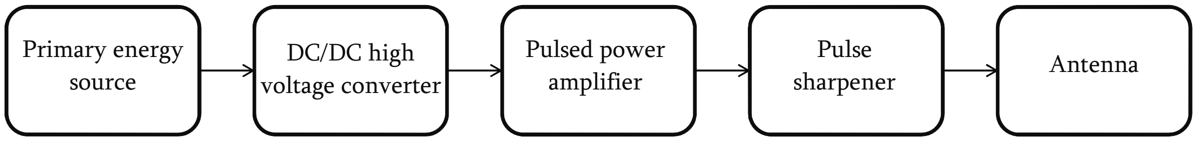

Figure 1. Synoptic of an electromagnetic radiative source

The dimensioning of a radiative source should be performed in stages, and in the opposite direction of the evolution of electric signals, that is to say starting from the load and back to the primary energy source. Indeed, once the characteristics of the load are defined, it is then possible to dimension the power amplifier and the power DC stage. Given their often mobile use these sources should be as compact as possible. This part presents various sources developed all over the world as a bibliographic study. To compare the sources efficiency, we propose to use a criterion: the "reduced figure-of-merit" (FOMr) (Eq. 1.) based on the figure-of-merit (FOM, i.e. r.E), the central frequency of the radiated field spectrum and the whole volume when an important integration was sustained. Since the dimensions of the antenna depend on the frequency of the wave to be radiated, we chose to take into account, in this criterion, the value of the center frequency of the radiated field.

$$FOMr = \frac{FOM}{V \times f_c} \tag{1}$$

With FOM: figure-of-merit of the pulse source (kV)

V: volume (L)

f_c: central frequency of the radiated field spectrum (GHz)

According to this criterion, the most powerful sources are generally those where integration efforts are most consistent.

All the sources presented here use for power amplifier a Marx generator or a Tesla pulse transformer. Their central frequency is between 120 and 1000MHz for volumes not exceeding 70 liters for the least compact sources.

2.1. ARC technology system

ARC Technology, US Army Space and Missile Defense Command and Texas Tech University have designed a tightly integrated and autonomous radio-frequency (RF) radiation system [1]. The final design includes batteries, power supply, Marx generator and plug and play helical or bicone antennas (Figure 2).

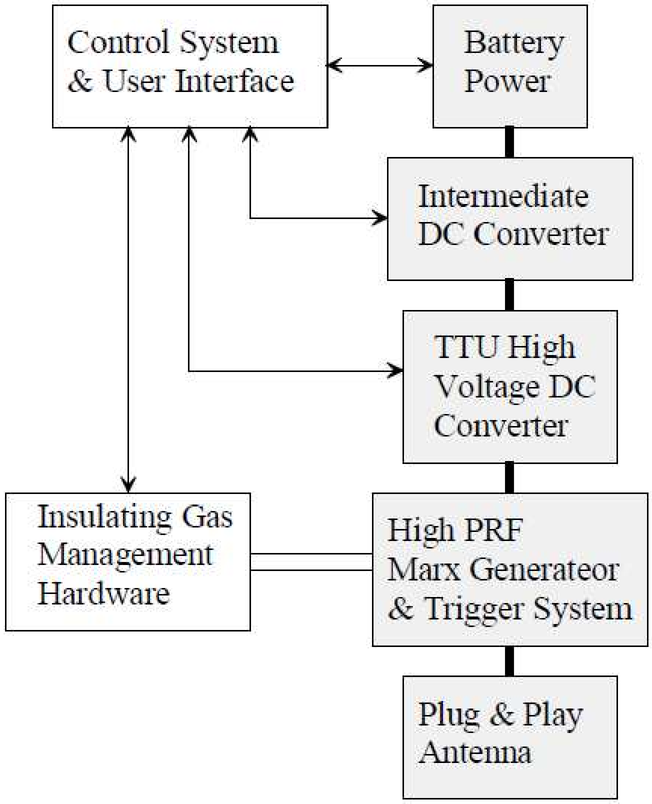

Figure 2. Block diagram of major subsystems

For cost and simplicity reasons, a 12V-12Ah sealed lead acid battery has been chosen. The intermediate DC converter raises the battery voltage up to 250V. To reduce mass and volume, the TTU rapid charger has an internal frequency of operation of 30kHz. This charger has demonstrated the ability to charge 50nF of capacitance up to 40kV at a repetition rate of 100Hz. The 15 stages Marx generator delivers 150kV with a 1.2ns risetime when driving a 50Ω load. The antenna is incorporated directly into the end of the Marx to maximize power efficiency and to minimize the overall system volume. A variety of antenna types have been designed and characterized, including helical and bicone configurations. Figure 3 shows the final package design with a helical antenna attached to the output end. Except for the antenna, the entire package has a volume of 28 liters.

Figure 3. Final RF radiation package with all subsystems

The radiated waveforms of a 1GHz helical antenna and of a 15cm bicone antenna (center frequency around 410MHz) achieve respectively 1500V/m and 4700V/m peak-to-peak at 10m. These results confirm that a helical antenna is not suitable to operate with a Marx generator without pulse forming stage. This remark is confirmed by the FOMr which is, respectively, around $0.5kV.L^{-1}.GHz^{-1}$ and $4.1kV.L^{-1}.GHz^{-1}$.

2.2. DIEHL systems

In cooperation with the German Government, Diehl BGT Defence has developed many technologies to deliver optimized High Power Electromagnetic pulses (HPEM). Typical development projects include the DS350 high-power laboratory source for electromagnetic effects testing, the DS110 range of compact sources, and ultra-high repetition rate UWB communication jammers [2]. The DS110 range of compact autonomous sources is available either integrated in small suitcases or in cylindrical geometry. Radiated field measurements will be presented to show that field strengths of approximately 100-160kV/m at 1m range are obtainable with a 350MHz damped sinusoidal pulse approximately 6ns long. For testing applications, the DS110B (Figure 4a) is tunable source, with a tunable center frequency range of 120-280MHz. The 41 liters DS110B suitcase includes an energy supply, a 50kV DC charger, a 6 stages Marx generator and a bicone antenna. In this configuration, the repetition rate is limited to 5Hz but, with an external charger (Figure 4b), the repetition rate can reach 140Hz. By using a simple add-on reflector, the maximum figure-of-merit is about 30kV and 105kV at, respectively, 120MHz and 280MHz [3] and the FOMr is, respectively, around $6.1kV.L^{-1}.GHz^{-1}$ and $9.1kV.L^{-1}.GHz^{-1}$.

(a) (b)

Figure 4. DIEHL DS110B suitcases

2.3. APELC systems

For about fifteen years, the Applied Physical Electronics, L.C. (APELC) [4] has focused on the research and development of compact geometry Marx generators used for dielectric material studies [5], for high power microwaves [6] or for X-ray generation [7]. More recently, APELC has proposed high power radiative systems driven by Marx generators. A 400MHz helical antenna driven by a 600kV Marx generator with a fast rising voltage of 80kV has a figure-of-merit of 50kV [8]. But the system with the best compactness is the EMP 2100 Series Suitcase (Figure 5), a computer and communications disrupter.

Figure 5. APELC EMP 2100 Series Suitcase

An LC resonator matched to dipole antenna is driven by a 300kV Marx generator to form a wide band radiative system. The radiated field at 1m can reach 125kV/m (Figure 6) at a 10Hz pulse repetition frequency (PRF) with 2 hours of autonomy. The spectrum central frequency is about 325MHz and the system volume is about 69 liters.

The electrical features are similar to the DIEHL ones, but with a bigger size. Its FOMr is around $5.6kV.L^{-1}.GHz^{-1}$.

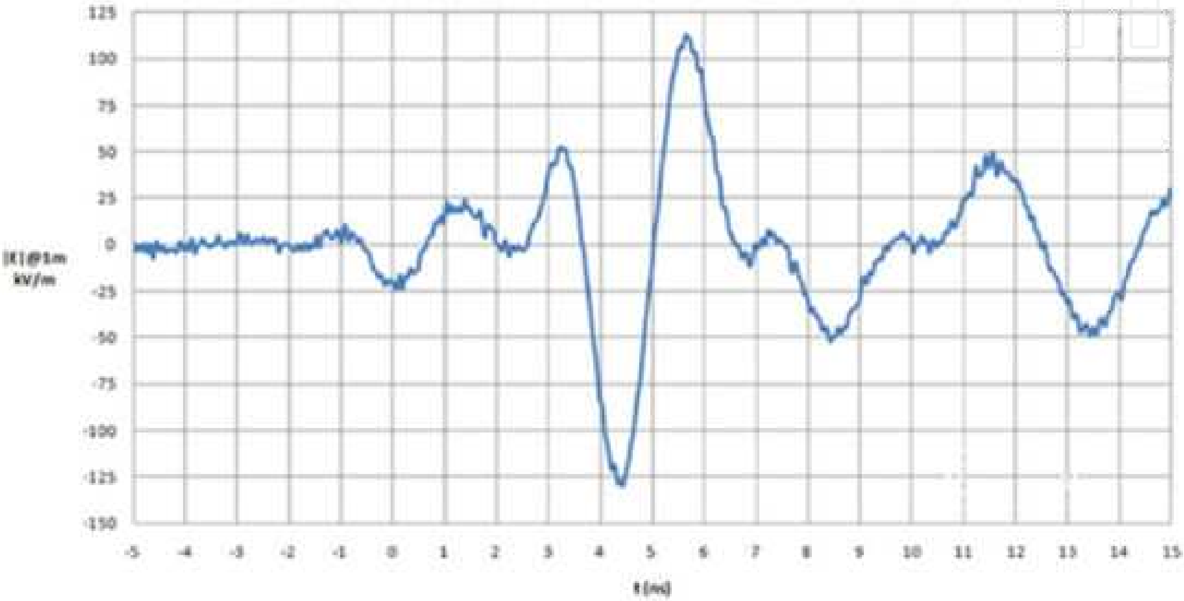

Figure 6. EMP Suitcase radiated electric field to a range of 1 meter [4]

2.4. DSTO – P^3G – DSTL systems

The previous systems use a Marx generator for the pulsed power generation. In 2002, the Australian Defence Science and Technology Organization (DSTO) presented a RF UWB source using a Tesla transformer [9]. The energy store and the antenna are combined in a single unit in the system design (Figure 7).

The antenna is charged to a high voltage, in the order of hundreds of kV, and then shorted at the bicone center by the spark-gap switch. To obtain about 100pF of capacitance, the interior of the structure has been filled with ethylene glycol and in order to increase peak radiated power, 1 m additional conducting elements must be attached to increase the effective radiating length of the structure. The measured radiated field at 1 m reaches 60kV/m with a 50MHz central frequency. But the volume of the system is not exactly known to calculate the FOMr. It is higher than 56 liters.

In 2005, the Plasma and Pulsed Power Group (P^3G) of Loughborough University presented an evolution of the previous system (Figure 8) [11] for the Defence Science & Technology Laboratory (DSTL).

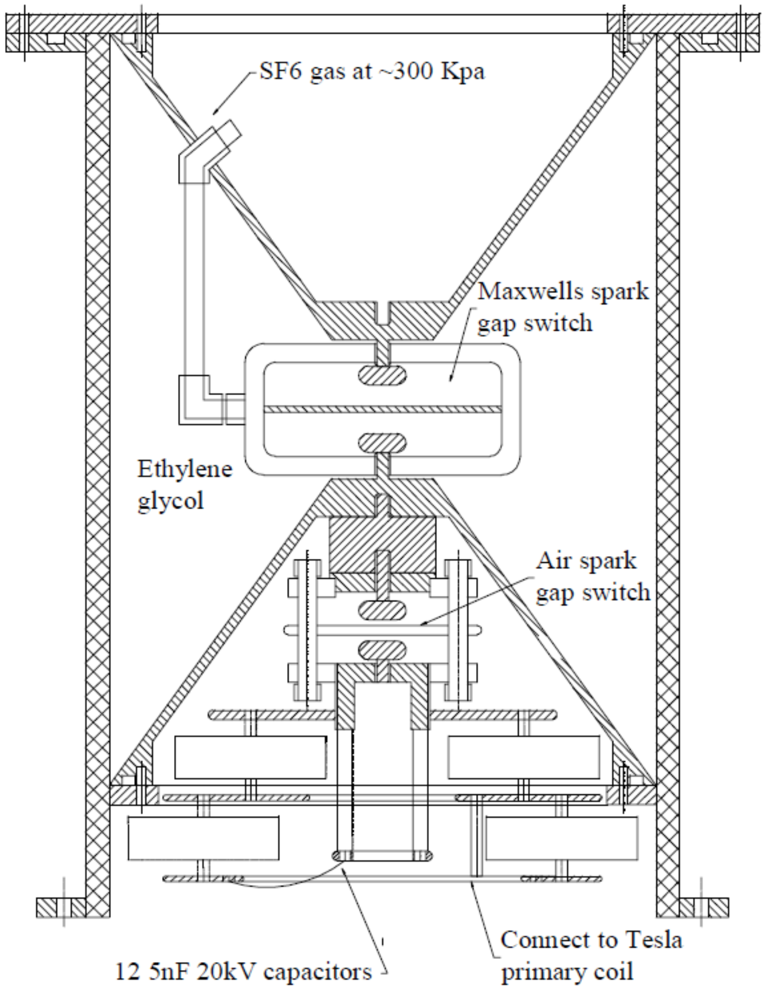

Figure 7. The biconical section of the high power source [10]

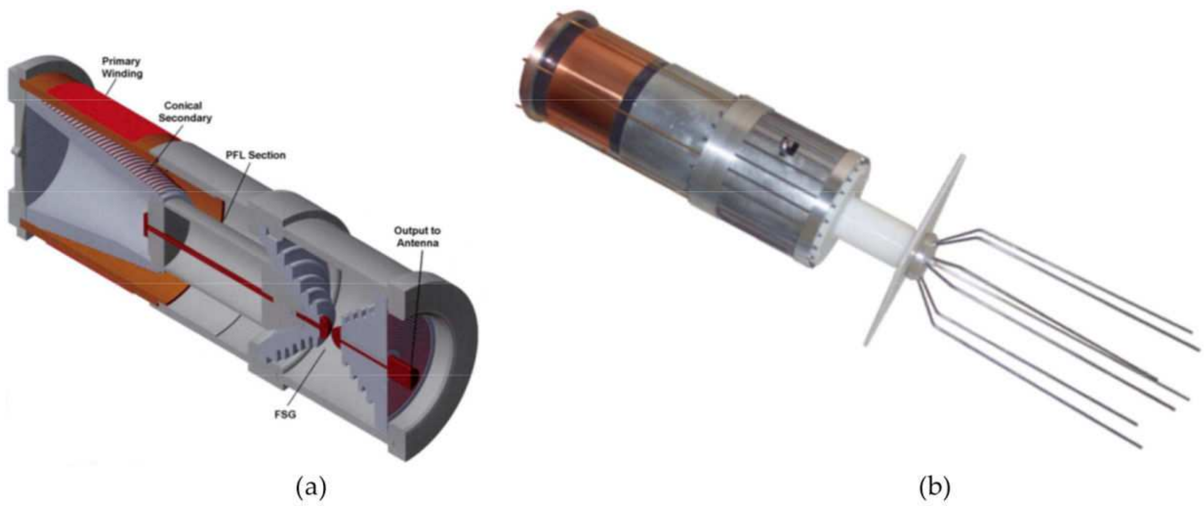

Figure 8. (a) Schematic of the system and (b) overall view of the system with the antenna

A 12V/30kV DC converter charges twelve 2nF capacitors. An oil insulated Tesla transformer, with a coupling coefficient of about 0.52, produces a 542kV voltage in a 60pF pulse forming line (PFL). This voltage is limited to 350kV for a 100Hz PRF. To minimize the volume of the system (70 liters), an omni-directional half wavelength dipole-type structure is used as a transmitting antenna, since it is both compact and radiation efficient. At a 5Hz PRF, the measured radiated field at 3m reaches 20kV/m with a 50MHz central frequency. Its FOMr is around $17.1 kV.L^{-1}.GHz^{-1}$. One year later, in the same volume, an improvement of the antenna and a greater Tesla output voltage allowed the measured radiated field at 10m to reach 12.4kV/m with a 75MHz central frequency (Figure 9) [12]. Its FOMr reaches $23.6 kV.L^{-1}.GHz^{-1}$.

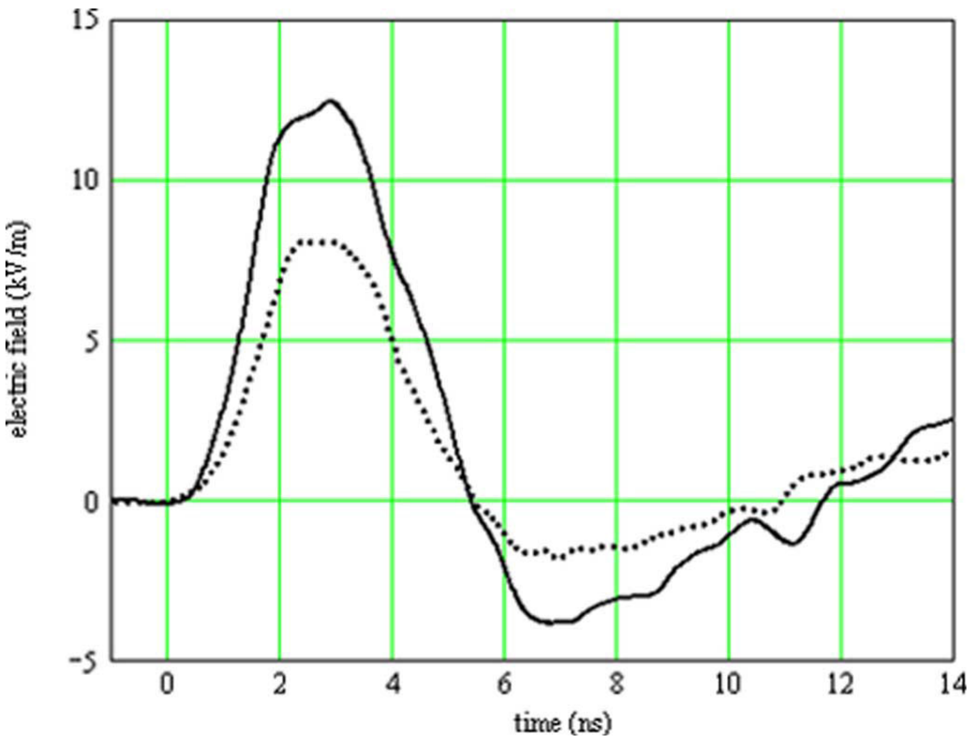

Figure 9. Radiated field waveform at 10 m (solid line) and 15 m (dotted line) from the source [12].

2.5. FOMr criterion comparison — Conclusion

This bibliographic study shows the diversity of these various sources developed all over the world. To compare the sources efficiency, we propose the FOMr criterion. The previous features are summarized in Table 1. The proposed FOMr criterion is calculated for all previous systems and their evolution. According to the FOMr criterion, the most powerful sources are generally those where integration efforts are most consistent.

This criterion allows concluding that a helical antenna does not fit very well with the use of a Marx or a Tesla generator without pulse forming stage. For this kind of antenna, the best antenna factor (i.e. rE/V) is obtained when the antenna is fed by a damped sinusoid [13].

System	Figure of merit (kV)	Central frequency (GHz)	Volume (L)	FOMr criterion ($kV.L^{-1}.GHz^{-1}$)
ARC (helical antenna)	15	1	28	**0.5**
ARC (biconical antenna)	47	0.41	28	**4.1**
DIEHL DS110B	105	0.28	41	**9.1**
DIEHL DS110B	30	0.12	41	**6.1**
APELC EMP Suitcase	125	0.325	69	**5.6**
P^3G – DSTL system	60	0.05	70	**17.1**
P^3G – DSTL system	124	0.075	70	**23.6**

Table 1. UWB systems features-Performances comparison

This criterion also allows us to conclude that if a certain compactness is expected, a pulse transformer should be preferred to a Marx generator, but with its inherent disadvantage of a slower voltage rise time being mitigated by use of a pulse forming line in conjunction with a high-voltage fast spark gap switch [12].

Taking into account of the central frequency in the FOMr in this criterion may suggest that it is better to radiate low frequency. Only the high frequencies are suitable to disturb or destroy electronics, the antennas are shorter and the system integration is easier. It is necessary to seek a compromise.

3. UWB Marx-based sources developed as electromagnetic jammers

3.1. Advantages of using an UWB source as jammer

High Power Microwaves (HPM) technologies generate a significant threat against target structures equipped with modern digital electronics. It is the goal of an HPM weapon system to interact with the increasing combination of soft and hardware functions in electronics. For affecting any target with such radiation, the frequency has to be matched to the frequency absorption spectrum of the target. Pulsed UWB radiation with pulse durations in the subnanosecond range do not need such matching to a single target. This assumption will be detailed in this part.

The advent of many UWB sources capable of producing output powers in the GW range allows managing real investigations of the susceptibility of electronic systems as well as their protection and hardening against such UWB threats. However, in the meantime, the development of very compact and autonomous UWB sources remain for real interests in the way to have at one's disposal, easy to use, transportable experimental devices.

In this context, two different sources were developed and their construction will be explained in parts 3.2 and 3.3.

3.2. Description of the first source developed for Thales Communications

This part aims at presenting the design and construction of an autonomous UWB radiation source developed for Thales Communication and consisting of a high gain broadband antenna driven by a subnanosecond pulsed power Marx-based source.

3.2.1. Description of the pulsed power source called "George"

A dedicated pulsed power source called "George" was developed in order to reach a few hundreds kV output voltages and repetition rate with a very competitive volume/power ratio. The original idea of this source was to directly integrate the pulse-forming device (a peaking stage and a crowbar switch) within the last stage of a Marx structure.

This generator is made up of a stack of ten vertical stages. Each stage consists of a capacitor, a set of stainless steel electrodes and a PVC disc. The energy is stored in HV 500pF/100kV DC capacitors through 33kΩ axial resistors. These ten capacitors are divided equally into two columns of five (Figure 10), which allows the loading time to be approximately halved in relation to a conventional structure (when the DC power supply is sufficient). Thus, the capacitors' charging time (to reach 99% of the maximum load voltage [14] is 2.3ms. In this configuration, the repetition rate limitation is 435Hz with no loss of output voltage (compared to single-shot mode operation).

Figure 10. Photograph of the generator equipped with its load and referencing resistors

Each spark gap is formed by two stainless steel electrodes. These ten horizontal gaps are adjusted by increasing the gap distance from the first to the last so that the generator switch is regular. Thus, the first stage has a 0.8mm gap and the last stage (largest) is set at 1.25mm. Their 5mm curvature radius means that we obtain a relatively homogeneous field in the insulating gap. The complete generator with the vessel represents a cylindrical volume of 20 liters (diameter=20cm and length=66cm).

This generator's main original feature lies in the design of its last stage, as represented in schematic form in Figure 11.

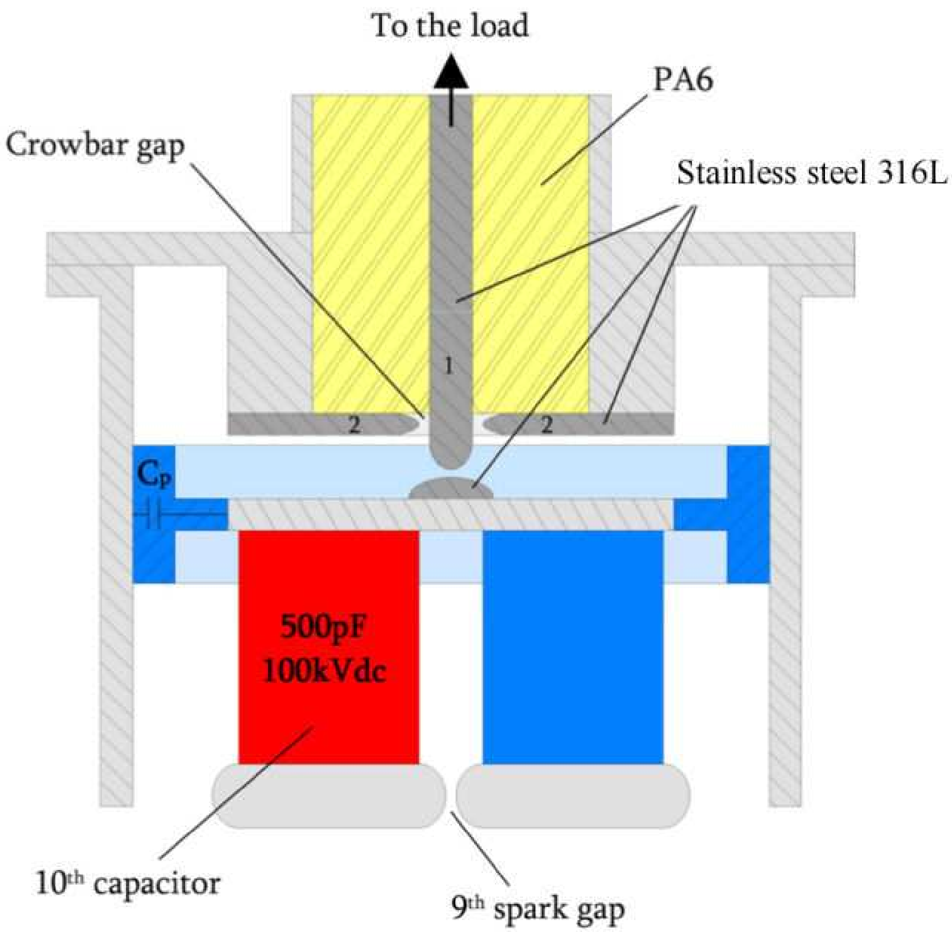

Figure 11. Diagram of insertion of pulse-forming line in the last stage of the Marx generator

The last stage was designed differently from the others in order to be able to insert a peaking capacitor (CP), which is necessary to obtain very fast rise times, and to match the output to a 50Ω coaxial line structure. This peaking capacitor is made up of a PVC component that is maintained between the electrode and the vessel enclosure. This component's geometrical dimensions are defined in such a way that it withstands the considerable dielectric constraints placed on this last stage, and in order to establish a low-value peaking capacitor (around 40pF).

Moreover, with a crowbar spark gap on the output electrode of the generator, it is possible to generate a subnanosecond pulse width based on the Marx-generated pulse. This crowbar switch allows the pulse's exponential decrease to be cut off. It is made up of two electrodes: the first electrode is the generator output (this is an HV electrode due to the switch in the last stage), and the second one (the ground electrode) is connected to the metal enclosure. This second electrode is a 5mm-thick stainless steel disc. After the crowbar, a coaxial line structure is directly integrated in order to avoid dispersion of the pulses' temporal characteristics.

A first set of experiments was carried out without the crowbar switch in order to determine the nature of the gas and the related pressure that would make it possible to reach output voltages with short rise times. The results of these different tests are set out in Figure 12. They were carried out in air and in an air-SF_6 mixture (75%-25%).

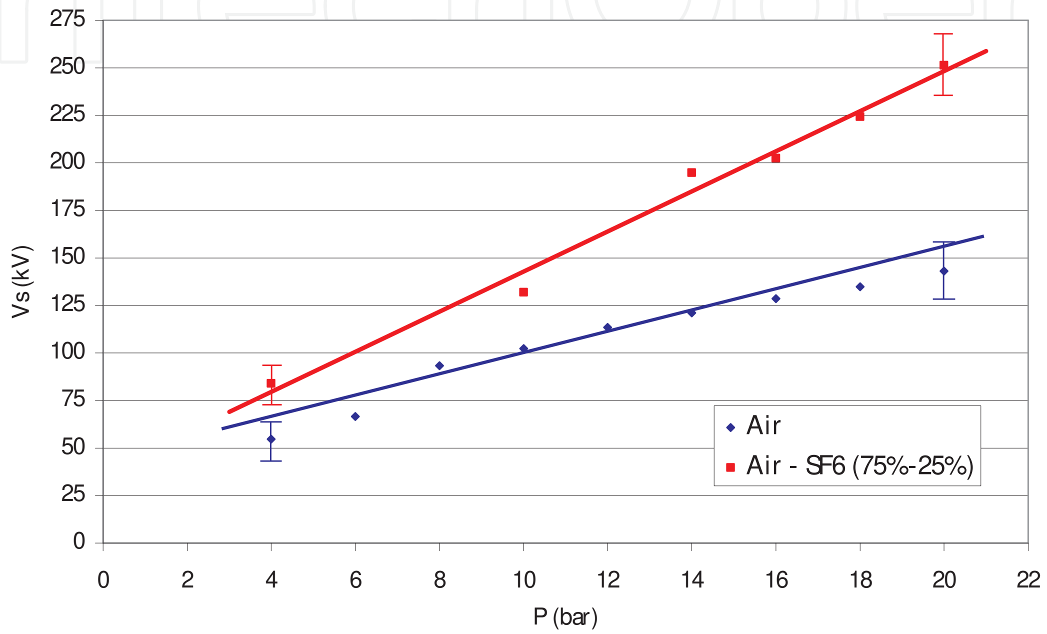

Figure 12. Output voltage versus pressure

For a set number of stages, the Marx generator output voltage increases according to the product pressure × the gap distance for a given gas. In this case, voltage amplitude can be adjusted to between 50kV and 150kV on a 50Ω load in air for pressures ranging between 2 and 20 bar. A small percentage of SF_6 (25% in this case) makes it possible to increase the amplitude of pulses by approximately 1.7 times in relation to those obtained with pure air. A 250kV voltage amplitude is obtained for a DC charging voltage of close to 50kV with 20 bar of pressure in this air-SF_6 mixture. For a maximum DC charging voltage of 100kV per stage, a 500kV amplitude pulse could be reached if the generator could withstand a pressure of 44 bar.

A similar study was carried out on the evolution of rise time in relation to pressure for these two gases. The results are shown in Figure 13. For each gas configuration, the shortest rise times are observed at the highest pressures. At a given pressure in the generator, air induces rise times that are shorter than in the air-SF_6 mixture [15]. The measured rise times lie between 250ps and 350ps in the air, and between 350ps and 500ps in the air-SF_6 mixture.

Figure 14 shows a typical pulse of the "George" generator. It is connected to a 50Ω coaxial line and to the "Valentine" HV antenna [16] (see part 3.2.2). First, the crowbar switch gap distance setting was tested to determine which solution leads to a breakdown in the rising edge of the

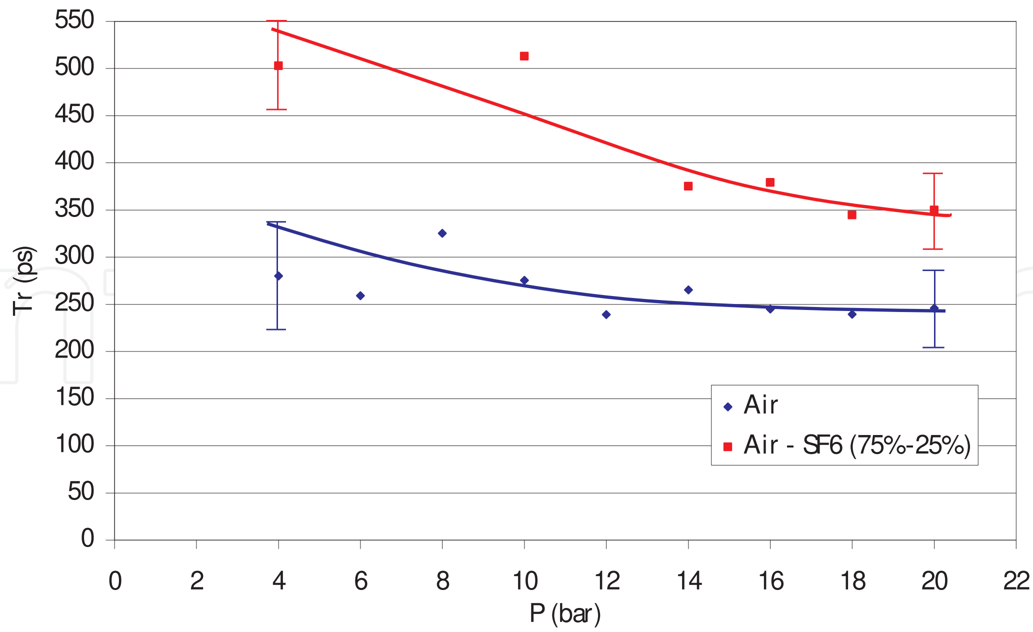

Figure 13. Rise time of the output pulses in relation to pressure

Marx-generated pulse. Thus, a 1.5mm distance seems to be the best configuration in order to obtain a subnanosecond pulse with minimized loss.

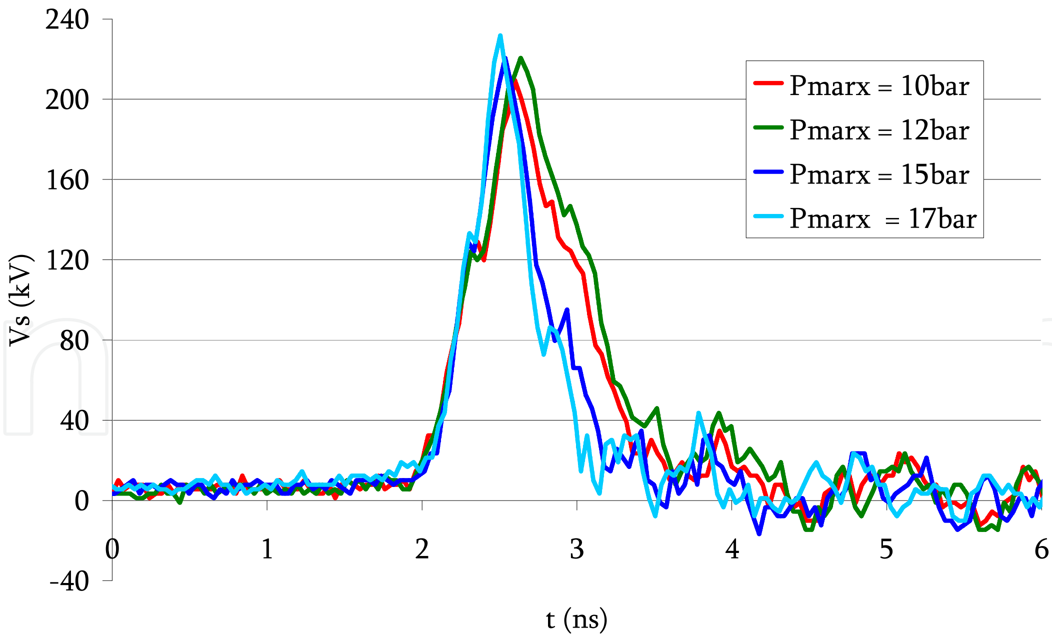

Figure 14. Marx generator output pulse shape (air-SF_6 mixture)

The pulse amplitude is 226kV, the rise time is 362ps and the mid-height width is 410ps for a 17 bar pressure. Tests were also carried out in repetitive mode operation. The DC HV charger available for these tests allowed us to test the generator up to a maximum repetition rate of 350Hz for an output voltage of 170kV on 50Ω. The tests were carried out by bursts of pulses that lasted a few seconds, separated by a few minutes of downtime.

3.2.2. Improvement of an existing UWB transmitting antenna

Another major factor in UWB radiation systems is the radiating element. The pulsed source is combined with a travelling wave antenna called Valentine antenna.

The pulsed power source, George, presented previously will be combined to a UWB transmitting antenna in order to radiate high electromagnetic fields. Due to its high gain and its capability to radiate short pulses without dispersion in the 300MHz–2.5GHz frequency band, the "Valentine" antenna, which was first used as a transmission antenna for a former radar application [16], was chosen to be the radiating element of our high-power UWB sources. The antenna was mechanically matched using CST Microwave Studio time-domain electromagnetic software to improve its dielectric strength. The antenna was originally composed of two metallic strips curved along a specific profile, and a 50Ω coaxial-to-stripline transition at the input. This structure is supported by two wooden side-pieces. Thus, this whole unit is 1200mm high, 1000mm long and 400mm wide.

We first focused on the development of the new coaxial-to-stripline transition. This transition was initially meant to transform (in air) a 50Ω coaxial transmission line geometry into a 50Ω stripline geometry located at the antenna input. Simulation work allowed us to modify this transition for our application with a very high voltage and very fast transients. When designing the transition, it is essential to take the bandwidth into account. According to Foster [17], the length of such a transition must be one quarter of the lowest-frequency wavelength. This length is fixed at 300mm. In addition, Farr in [18] also gives a simple formula concerning the rise time that can be preserved in such a transition as a function of several transition dimensions:

$$t_r = \frac{\pi^2}{2} \frac{\sqrt{\varepsilon_r}\left(\frac{D}{2}\right)^2}{lc} \tag{2}$$

where ε_r is the relative dielectric permittivity of the insulating material, D is the inner diameter of the output conductor on the coaxial transition part, l is the transition length and c the light velocity. From (2), the selected dimensions and the use of “Univolt” oil with a relative permittivity of 2.3 gives a 105ps rise time, which is in accordance with the power sources' time-dependent parameters.

A PVC part was then inserted between the two strips and was extended from the new transition up to the end of the antenna to ensure good dielectric insulation for the high-voltage pulses. CST Microwave Studio software was used as a design-support tool. The design of this modification, its shape and its influence on the antenna's electromagnetic characteristics were studied. The complete design of the HV antenna is shown in Figure 15.

The HV antenna was studied in the 0-3GHz frequency band. A Gaussian pulse, with a frequency spectrum larger than that of the antenna being studied, is used as the input signal for the time-domain simulation, which seems to be the best solution in order to study the calculation of the S_{11} parameter. The input port is defined on the coaxial part of the transition.

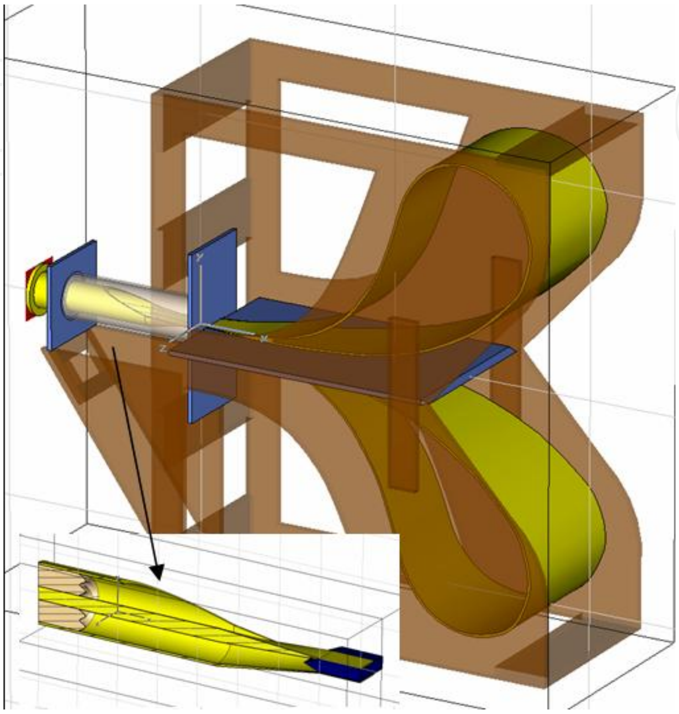

Figure 15. 3D modeling of the "Valentine" HV antenna and the "Tulipe" transition

Figure 16 shows the measured S_{11} reflection parameter of the modified antenna. This result is compared to the calculated S_{11} parameter in the 300kHz-3GHz frequency range. Results are quite similar. Except for 600MHz, the S_{11} parameter is less than -10dB between 300MHz and 3GHz.

The new HV antenna's measured gain up to a frequency of 3GHz is shown in Figure 17. This response is compared to the calculated response, as well as to the measured gain of the original low-voltage antenna. Both of these are realized gains, which take account of the matching of the antenna.

It has been shown in [19] that the wooden structure of the antenna is responsible for the gain drop to below 10dB between 800MHz and 1.6GHz. A parametric study was conducted on the variation of the wood's relative permittivity value using CST, and we have concluded that a structure with a lower relative permittivity (for instance, ε_r=2) could reduce this drop and stabilize the gain at around 10dB within this frequency range. Totally avoiding using a wooden structure would make it possible to obtain a more satisfactory result.

The measured and calculated radiation patterns in H and E planes at 500MHz, 1GHz and 2GHz are shown in Figure 18 (a)-(f).

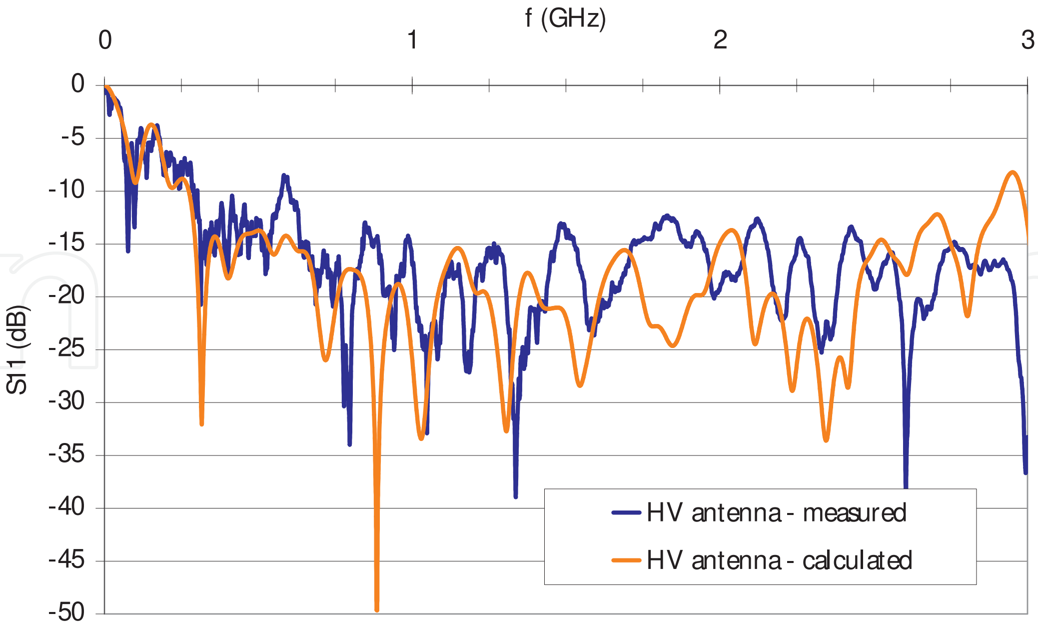

Figure 16. S_{11} parameter of the new "Valentine" HV antenna

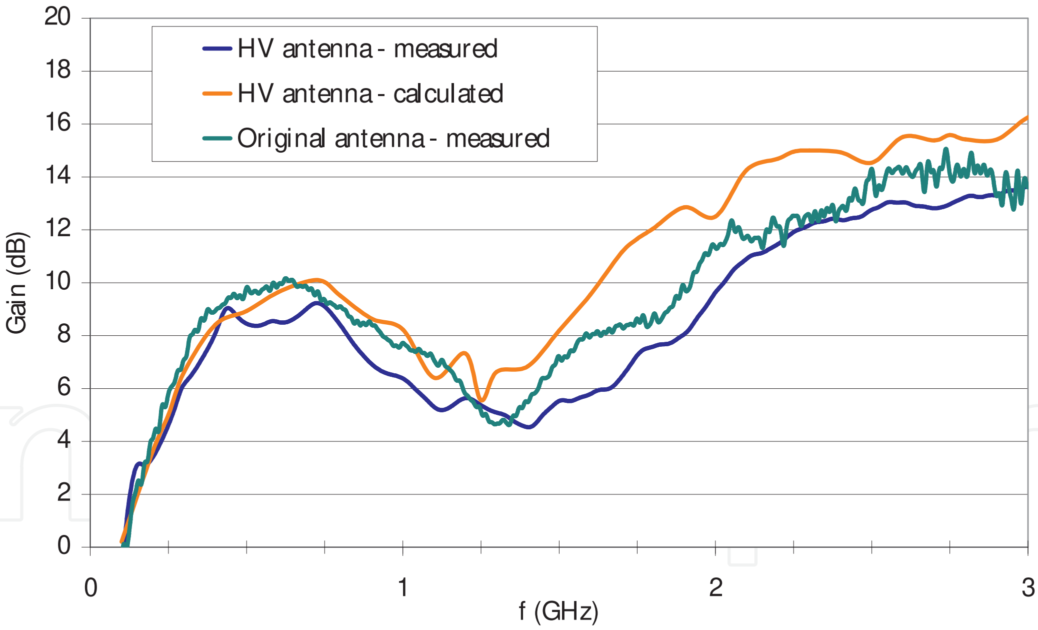

Figure 17. Realized gain of the "Valentine" HV antenna in the axial direction

Good agreement is obtained between the theoretical results and the experimental results. In each plane, the radiation patterns become narrower as the frequency increases. The backwards radiation is greater at the lower frequencies. This is due to the fact that the low-frequency parts of the current pulse are reflected at the end of the antenna and propagated towards the end of

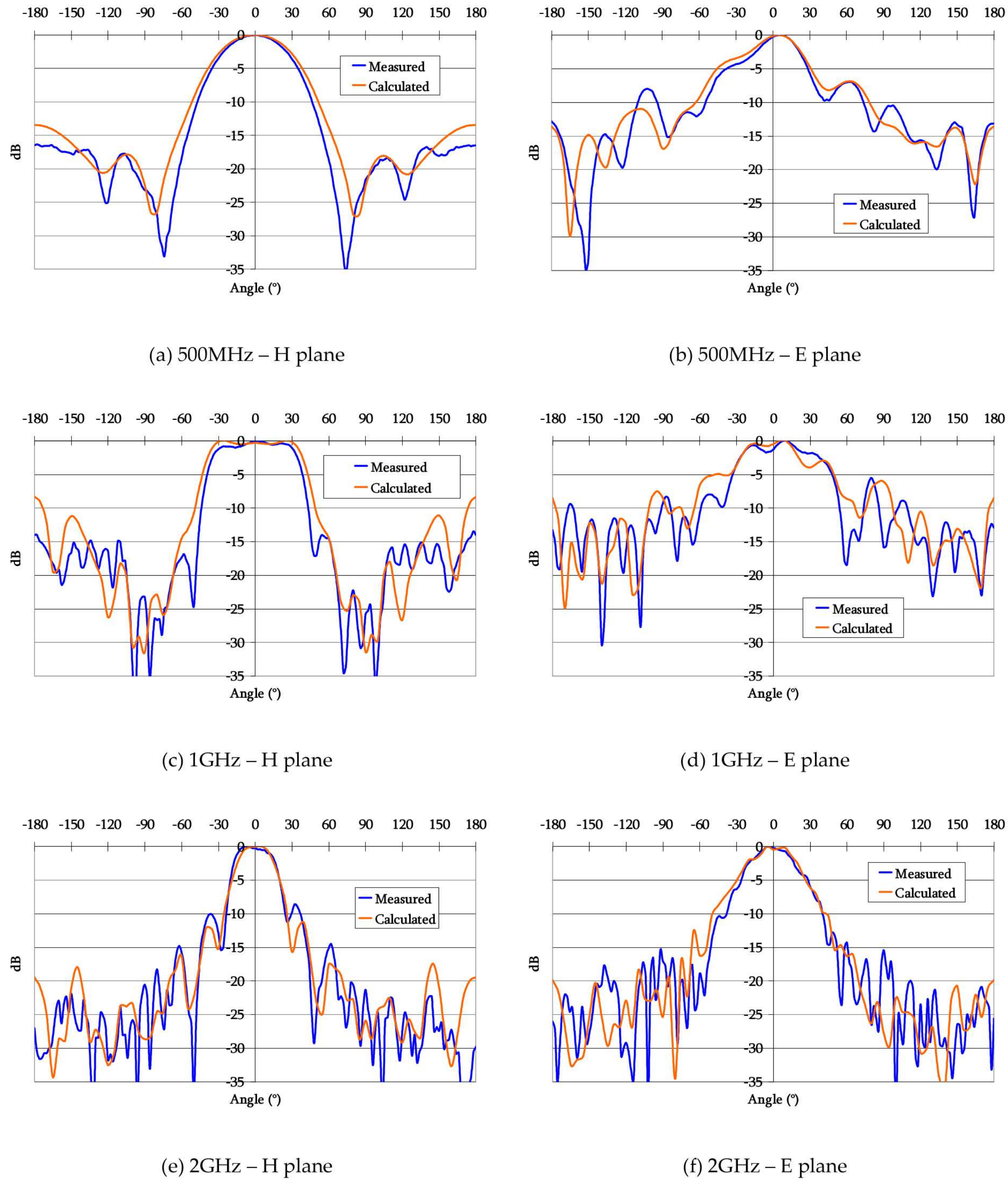

(a) 500MHz – H plane

(b) 500MHz – E plane

(c) 1GHz – H plane

(d) 1GHz – E plane

(e) 2GHz – H plane

(f) 2GHz – E plane

Figure 18. Radiation patterns in H and E planes at 500MHz (a),(b), 1GHz (c),(d), 2GHz (e),(f)

the metal strips. On the contrary, high frequencies are radiated before reaching the end of the antenna. The backwards radiation is lower than -20dB for frequencies greater than 1.5GHz. Moreover, the main lobe is narrower in H plane than in E plane. The directivity of the antenna in this plane depends on the width of the metal strips. The wider the strips, the greater the antenna's directivity in H plane.

3.2.3. Experimental tests of the Thales communication's pulsed radiation source

Various tests on the whole source (battery-DC/DC converter-Marx generator-pulse forming device-antenna) were investigated in order to evaluate the figure-of-merit of our system (Figure 19). In this section, we present different experiments that aim to determine the amplitude and temporal characteristics of the electric field that is radiated along the axis of the "Valentine" antenna when it is associated with each of the two pulsed high-voltage sources presented above. Two methods of measuring the field are studied: a direct measurement using a derivative field sensor, and an indirect measurement of the field diffracted by a sphere (the "MICHELSON" method) [20-21].

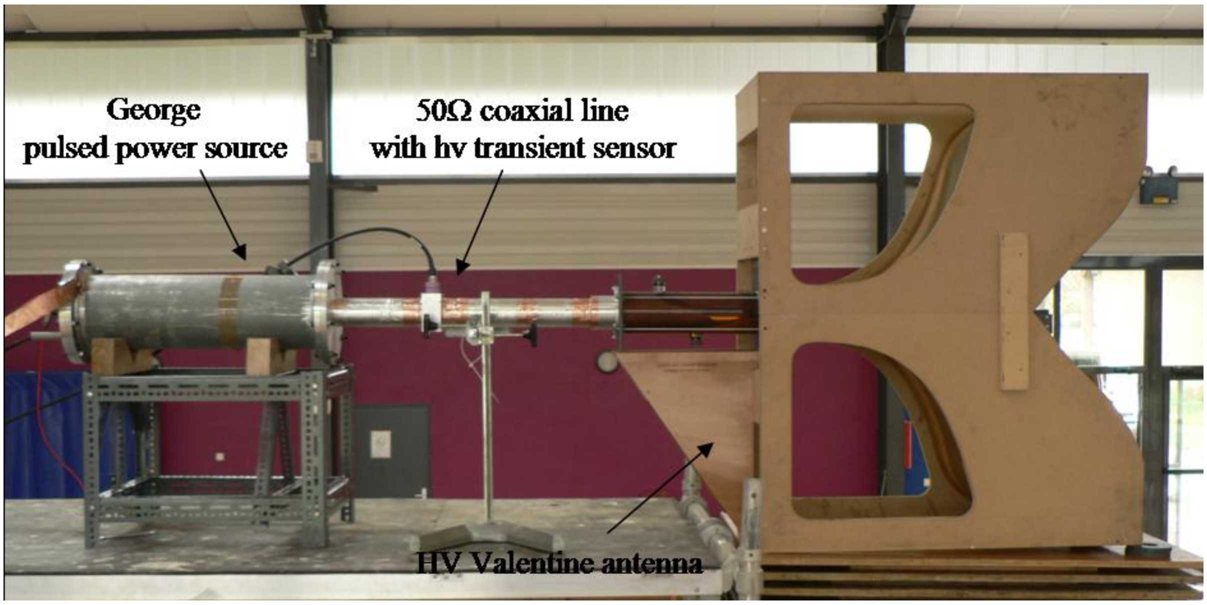

Figure 19. First repetitive high-power ultra-wideband source

The XLIM Laboratory of Limoges University has developed a new method for measuring intense electromagnetic fields called the "MICHELSON method". This name is the French acronym for Instantaneous ElectroMagnetic Field Measurement by Signature of a Neutral Object [21]. The principle is based on the use of a target which scatters the electromagnetic field whose characteristics we are trying to find out. We then measure the scattered field in a given direction with a conventional antenna that is adapted to the field bandwidth. The purpose is to come back to the incident field from the output antenna voltage. With this method, high power sources can be studied with simple equipment because there is no risk of breakdown. The conventional receiving antenna recovers only a fraction of the incident field and the target is insensitive to this. As the target is small in size and no cable is used, disturbances are also limited with this measurement system.

Figure 20 represents the evolution of the radiated electric field measured by the antenna, which has been extrapolated to 1m using this method.

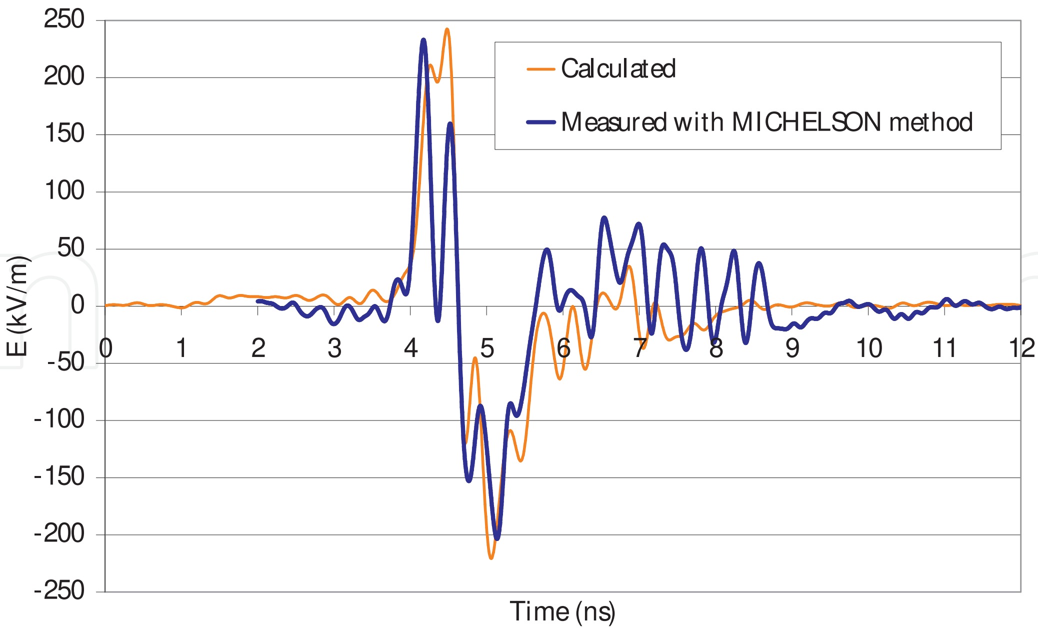

Figure 20. Comparison of measurements using the "MICHELSON" method and calculated radiated fields

The metal sphere target (diameter of 24cm) is located at a distance of 5m from the emitting antenna. The receiving antenna is a UWB antenna developed by XLIM whose bandwidth lies between 300MHz and 3GHz. The result of this measurement is compared with a theoretical estimation. The figure-of-merit value of the radiated field measured using this method is 436kV, with a positive amplitude of 233kV and a negative amplitude of-203kV. The impulse width is 1.82ns. The theoretical estimation gives an estimated value of 460kV. The results obtained by this method of measurement are thus very close to those estimated by calculation.

Its FOMr reaches 2.1kV.L^{-1}.GHz^{-1}.

3.3. Description of the second source developed for the French Ministry for Defense

In the same context, the DGA (French Ministry of Defense) wanted to dispose of an ultra compact UWB source capable of figure-of-merit of hundreds of kilovolts in a repetitive mode of operation. The FOMr would be drastically improved. Four French entities (the CEA, TECHNIX, XLIM, CISTEME and the University of Pau), developed a tightly integrated unit, including a battery pack, an intermediate DC/DC converter, a high voltage DC/DC converter, the control system, a high pulse repetition frequency (PRF) Marx generator with its integrated pulse forming unit and a deployable UWB Valentine antenna.

3.3.1. Compact and self-contained 50kV/100Hz power supply

This high voltage power supply is made of four modules: the battery power source, an intermediate dc/dc converter, a high voltage dc/dc converter and a control system. The whole modulator is included in a metallic electromagnetically tight suitcase which represents a volume of 10.4 liters (390 × 280 × 95 mm).

The battery module performance clearly dictates upper theoretical limits to both the maximum average power and overall energy that can be delivered by the high voltage power supply. Li-polymer battery offers the best power density. We have chosen to associate six 7.4V/1350mA.h battery units in a series/parallel arrangement to create a 16.8V/1.5kW DC primary source. These batteries permit to achieve, in real experimental conditions, autonomy of more than 35000 shots.

This primary power source is associated to an intermediate DC/DC converter to raise the battery voltage up to the voltage level required by the high voltage dc converter, typically 300V to 380V. This intermediate converter is designed as two halves standard H bridges in parallel operating each other at 20kHz to drive a transformer. Corresponding outputs (on the each secondary winding) are then rectified and added to achieve a nominal 350V/700W DC output with a power efficiency of 90 %. The electrical circuit structure of this converter is classical, but special efforts were made on the choice of semi-conductors and the arrangement of components to avoid heaters and cooling system, to improve the size and volume of the overall converter and to limit losses. This converter can sustain an average power of more than 700W for some tens of seconds.

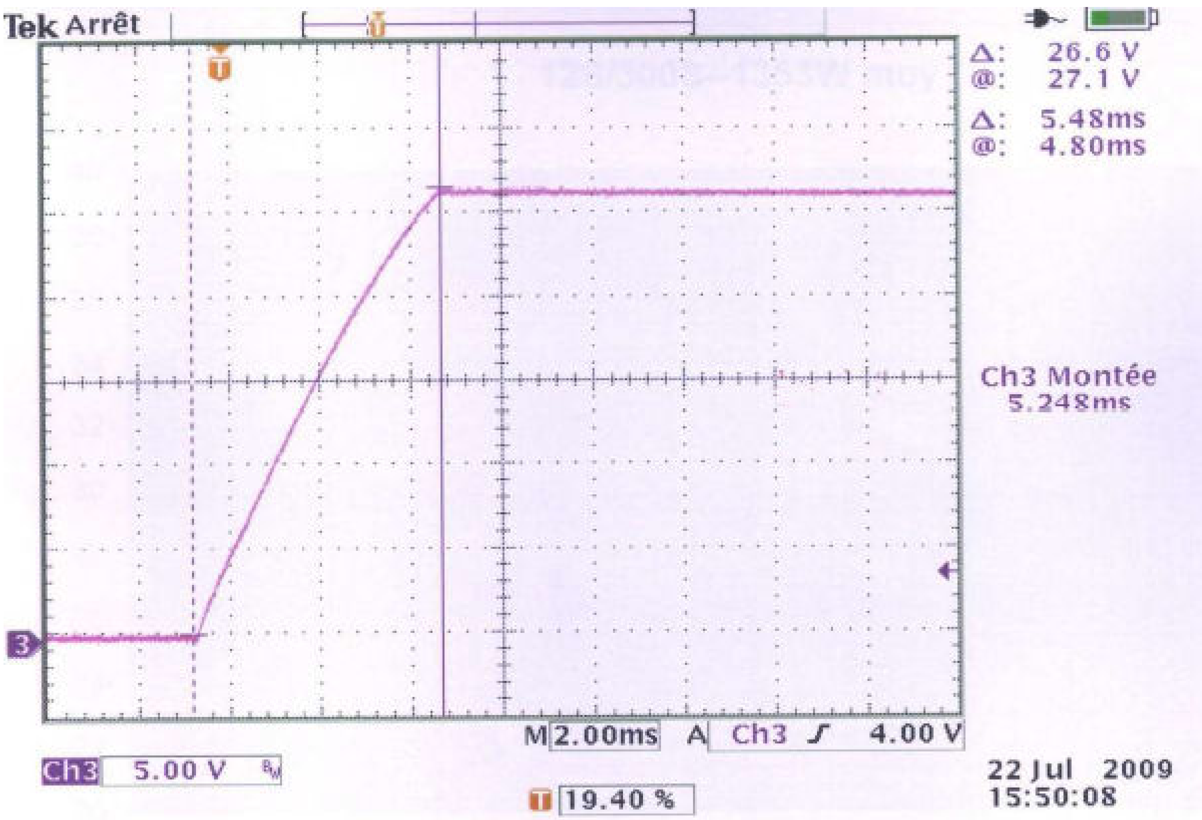

Figure 21. Rapid charging of a 5nF capacitor (equivalent capacitance of the Marx generator) in 5.2ms at 50kV. Input voltage : 370Vdc

The high voltage DC converter is an IGBT H-bridge which drives the primary side of two transformers from the DC output voltage of the intermediate converter. Secondary windings of the transformers are fed into a capacitor-diode multiplier to achieve its 50kV output. Figure 21 shows results of a 370Vdc test on a 5nF capacitor representing the equivalent capacitance of the Marx generator. This charger has demonstrated its ability to charge 5nF of capacitance up to 50kV in 5.2ms at a repetition rate of 100Hz, which corresponds to 1.2kW of average power from an input voltage of 370Vdc. This HV converter represents a volume of 5.5 liters (270 × 254 × 77 mm). The biggest mass and volume reductions from classical designs were achieved by considering an instantaneous peak power operation during burst sequences of few seconds where no current regulation is required. As a consequence, heater and cooling system were removed, IGBT were mounted on the metallic box containing the capacitor-diode multiplier, and other solutions were brought in the same way.

An on-board control system, based on the use of a microcontroller PIC sets the operating conditions: burst parameters (number of shots and repetition rate) and the sequencing of a shot (start/stop of the intermediate converter, H-bridge electronic command, HV inhibition...). For tests, it is coupled to a remote control interface by an optical fiber at a distance up to 75m. It permits to drive the system securely and to benefit of a monitoring of the system operation (battery status, voltage data…).

3.3.2. The compact Marx generator with its integrated pulse-forming unit

The Marx generator was designed from the experience of previous projects [22]. It is made of eight stages employing spark gap switches, pressurized in pure air, and 560pF/50kVdc ceramic capacitors (Figure 22).

Spark gaps are made of two stainless steel spheres screwed in a Plexiglas tight cylinder. The charging and discharging resistors have been replaced by ultra-compact inductors (two inductances of a few tens of μH per stage) for rapid charging. Indeed replacing the classical resistive components of the Marx by charging inductors is imperative for repetitive operation at pulse repetition frequencies of about 100Hz. All the inductances are insulated with dielectric oil which allows a maximum DC voltage applied about 45kV.

These eight stages are vertically piled up in a cylindrical PVC tight enclosure filled with oil. Package dimensions for this Marx generator are 175mm in diameter and 396mm in length. That means, with the integrated pulse forming line a volume of 9.5 liters.

The last stage was differently designed compared to the others in order to be able to insert a peaking capacitor, necessary to obtain very fast rise-times, and to match the output at a 50Ω coaxial line structure (Figure 23). With the integrated PFL the length grows to 463mm. The functioning of this peaking capacitor is carried out by using a PVC torus, maintained between the electrode and the vessel enclosure. The geometrical dimensions of this disc are defined in order to comply with the important dielectric constraints of this last stage and to establish a low value peaking capacitor (around 40pF). Moreover, with a spark-gap crowbar on the output electrode of the generator, it is possible to generate a subnanosecond width pulse based on the Marx generated pulse (Figure 23). This crowbar switch allows the exponential decay cutting of the impulse.

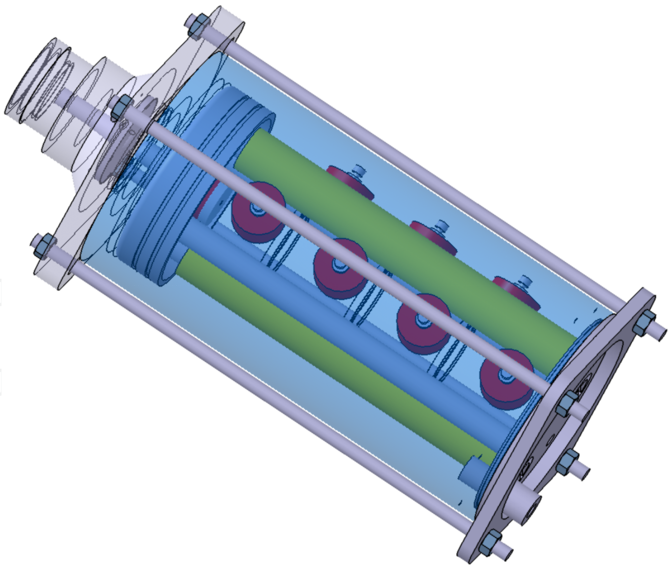

Figure 22. The compact Marx generator with its own forming unit

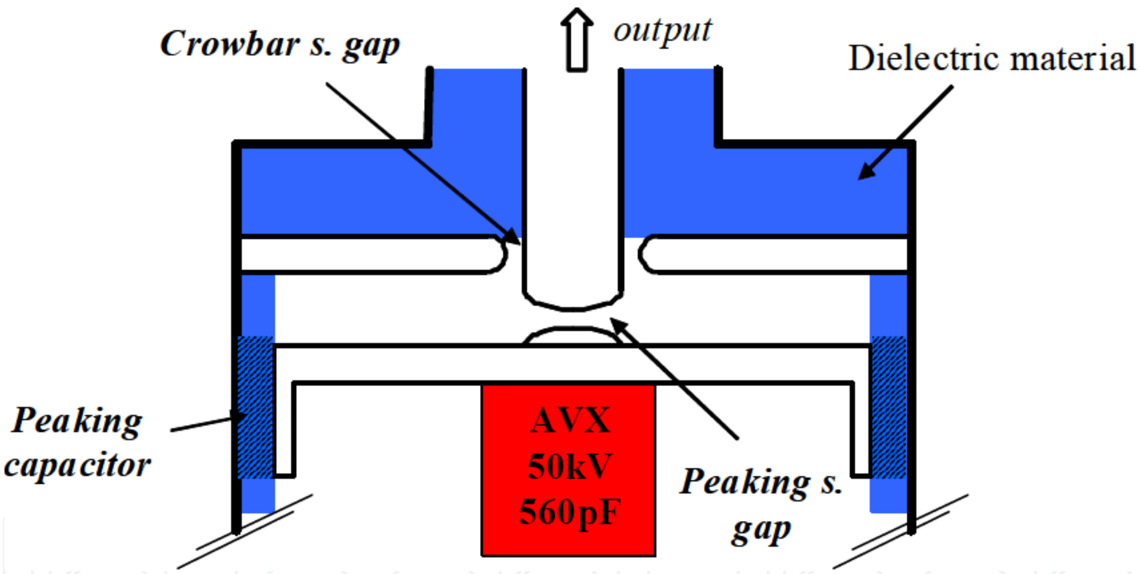

Figure 23. Principle scheme of the pulse forming unit

Mechanical tests certified the device up to 5bar in the Marx chamber and 30bar in the peaking chamber. Tests were carried on up to 4bar corresponding to a charging voltage closed to 40kV which could be damaging for inductance in repetitive operations. The pressure in the PFL is adjusted to 22bar. In these experimental conditions, the rise-time due to the peaking switch is about 700ps and the fall-time (20%-80%) due to the crowbar switch is about 200ps. The peak voltage obtained during this test is about 140kV. Repetitive tests were limited to 140kV and 100Hz. Figure 24 presents a short burst of 100 shots at a 140kV output magnitude for a 100Hz PRF. The maximum voltage gradient is 117kV in 330ps which represents $\Delta V/\Delta t = 3.55 \times 10^{14}$V/s.

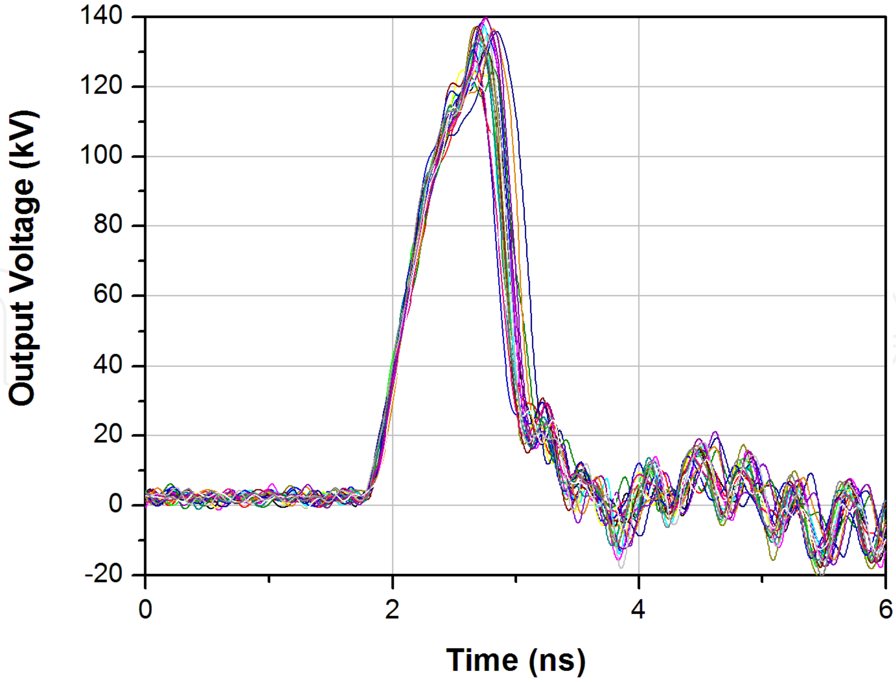

Figure 24. Output signal on a 50Ω resistive load during a 100Hz burst for P_{MARX}=4bar, P_{PFL}=22bar (air/SF_6 mixture), d_{PFL}=1.5mm, $d_{CROWBAR}$=1mm

3.3.3. The whole radiating source and its performances

The pulsed power generator previously presented is combined to a new UWB travelling wave transmitting antenna to radiate high electromagnetic fields [23]. This antenna is deployed when used and can be folded when the system is not used. It is made up of a coaxial-to-stripline transition and two metallic strips curved along a specific profile (see Figure 25).

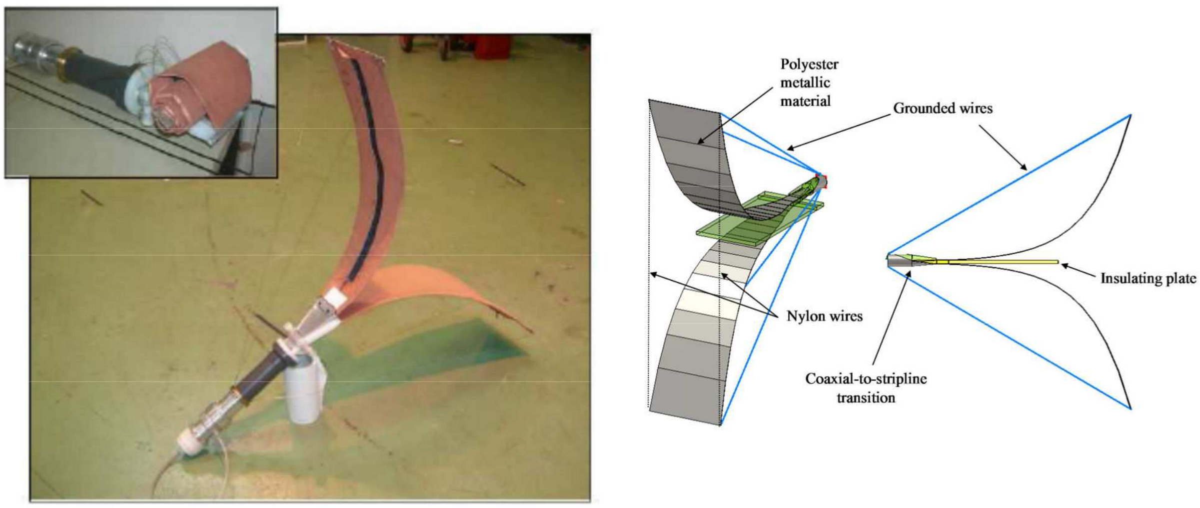

(a) (b)

Figure 25. Deployed Valentine antenna [23]

The system is supplied by the self-contained 50kV/100Hz modulator and radiates electromagnetic field by means of the deployed Valentine antenna. The measured field has a width of 3.58ns, a positive amplitude (reduced to 1m) of 193kV/m and a negative one of 122kV/m. Then, the figure-of-merit value of the radiated field is quite below 200kV. The spectral density is distributed from the DC frequencies to 1.2GHz (at -20dB of the maximum).

According to our "reduced figure-of-merit" criterion, the FOMr factor of our UWB Marx-based source is FOMr=16kV.L^{-1}.GHz^{-1}.

4. PULSAR a synthetic aperture radar for landmine detection

4.1. Advantages of using an UWB source as radar

The demand for switch closure on sub-nanosecond time scales has arisen in a range of applications including high power microwave or pulse laser drivers. That is why ultra-wide band microwave sources and antennas are of interest for an application such as transient radar. One of the most promising missions of such potential radar is the detection of buried and surface land mine targets. In order to detect foliage and ground concealed targets, UWB short pulse radar seems to be of the emerging solution.

An extremely short pulse generated by a source is transmitted through a transmit antenna, interacts with dense media and objects ahead, and radar returns are captured with a receive antenna and sampled. To enhance discrimination between targets and clutter, the excitation should be as wide band as possible. However it is also essential to operate at frequencies for which adequate soil and foliage penetration can be affected. The upper frequency band is useful to improve the spatial resolution whereas the lower frequencies are needed for the penetration through foliage and into soil. The device must transmit and receive waveforms with usable bandwidth from 200MHz to 4GHz.

The usable range of UWB radar is ultimately dependent upon the peak power of the transmitted pulse and the pulse repetition rate, which define the total energy transmitted in a given period, while the range resolution is dependent upon the rise-time and duration of the transmitted pulse. That is why a fast rise-time is needed to detect objects with small size: the discretisation is improved as the bandwith is increased.

4.2. Description of the very compact source based on pulse forming structure

This part is dedicated to the presentation of the development of a fast compact pulse generator used as the generation system of an UWB synthetic aperture radar device called PULSAR (Figures 26 and 27) for the French Technical Centre for Armament Electronics (CELAR).

So a UWB coaxial pulse generator is used for the peaking function. The object is to pulse sharpen the output of a first device in order to generate a very fast repetitive voltage pulse. For this function, the technology concerning a high pressure gas switch in the coaxial generator is largely used [24] because the gas quickly regains its dielectric strength after the discharge

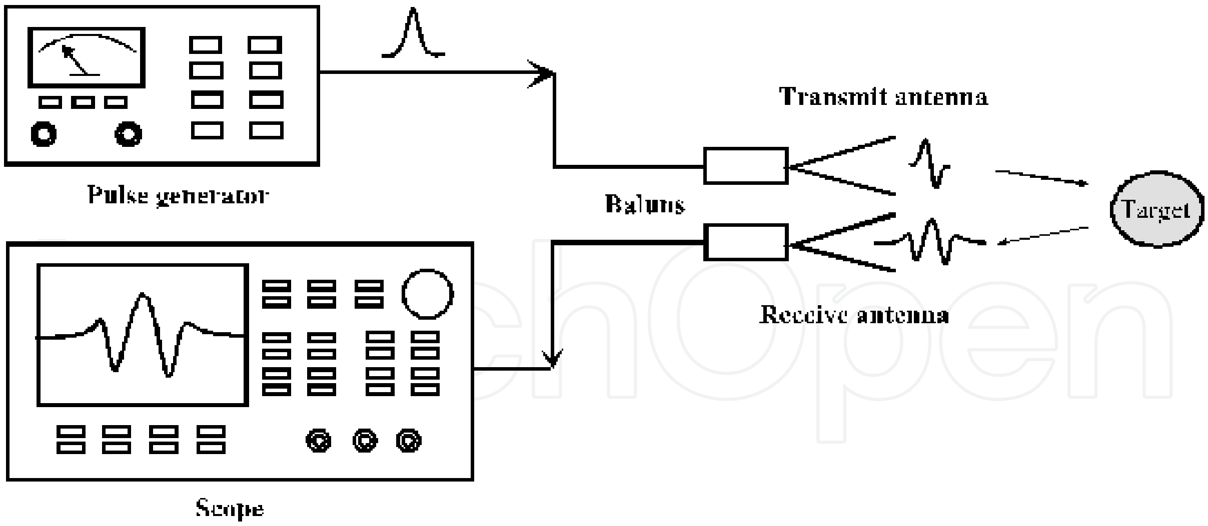

Figure 26. Schematic representation of the UWB synthetic aperture radar called PULSAR

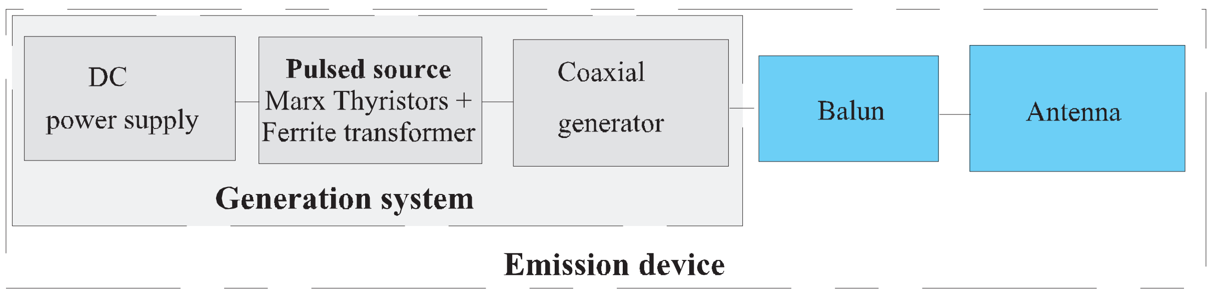

Figure 27. Basic structure of the emitting source

and the dielectric withstand of gas allows very interesting voltage levels. This technology can be easily designed for the sub-nanosecond time scales, and the ratio between the parasitic inductance generator and the geometry impedance can be reduced enough to generate sub-nanosecond rise-times.

The complete generator can be suitable for UWB radar applications provided that the output pulses reproducibility obtained is good (±5% or less). The coaxial generator needs a pulsed source to improve this main characteristic (Figure 27). The aim is to lead to the breakdown of the high pressure gas switch during the rise of the pulsed source voltage output. In these conditions, the time allowing to find an initiatory electron is very short (<100ns) and the stability and the reproducibility of the output pulses are improved. In this case, the breakdown of the coaxial generator gap will occur at the same voltage level and the output voltage amplitude is always similar. This source must generate pulses with fast rise-time and amplitude twice higher than the coaxial generator one.

The generation system associates four power modules (Figure 28): a 1kV DC power is used to supply a Marx generator; a ten-stage Marx generator using thyristor switches can generate pulses of about 10kV; a pulse transformer using the magnetic properties of ferrite cores allows to amplify the 10kV pulse to reach 60kV and a coaxial generator used as a pulse forming line to sharpen the pulses.

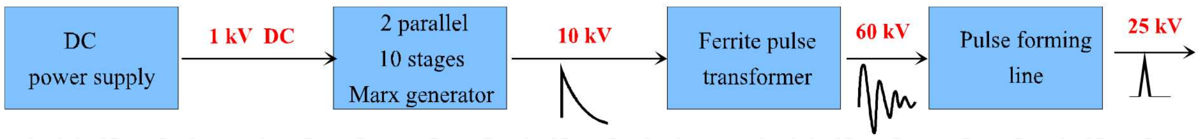

Figure 28. Schematic representation of the generation system

Usually, a Marx generator forms the first section of the energy storage system in most experimental set-ups. For the switching function, thyristors were chosen. They offer a perfect discharge allowing high repetition rate with weak jitter, considerable output voltage and fast rise-time sufficient for our application. One thyristor 30TPS16 from IRF is used by stage.

First experiments have shown that to obtain a good yield between the output of the Marx generator and the pulse transformer, an energy value of 110mJ is required at 7kV. That is why we designed and built a generator containing 2 parallel Marx circuits, to limit the current value on each thyristor. To reach the energy value required, each Marx circuit is made of 10 stages loaded at 1kV with 22nF capacitors per stage (the equivalent output capacitor is 4.4nF).

Therefore the input capacitor is 44nF. The schedule of conditions requiring a 500Hz behavior, the generator's DC supply must therefore supply a 400mA current, 1kV source. However this high value current value leads to thermal dissipation problems in the Marx resistors. As a result, all the resistors of a standard Marx generator were replaced by diodes. In these conditions, the Marx generator only works if it is connected to its output impedance, i.e. the pulse transformer. A pulse transformer using the magnetic properties of ferrite cores is used to reach 60kV. The tests and description concerning this pulse transformer can be observed in [15].

Finally, the main characteristics of the pulsed source are summarized in Table 2:

Input Transformer Voltage	7kV
Output Transformer Voltage	60kV
Transformation Ratio	8.6
Rise-time (10%-90%)	250ns
Width (50%)	500ns
Repetition Rate	500Hz

Table 2. Main characteristics of the pulsed source

To achieve energy compression (to enhance the pulse power by decreasing its duration) as well as to shorten the rise-time, the energy from the pulsed source (Marx generator associated with pulse transformer) is fed into a coaxial pulse forming line. This generator (Figure 29) is made of a 50Ω coaxial pulse forming line charged by the pulsed source through a resistor, a high pressure gas switch and a transmission line impedance adapter equal to its characteristic impedance. The high-pressure gas switch is then switched on and a pulse is generated due to the boundary conditions (Zin → ∞ and Zout=50Ω). Theoretically, under these conditions, high-voltage square pulses are produced with an amplitude equal to half of the charging voltage value. The duration of the output pulse is equal to twice the one-way wave transit time in the pulse forming line. The fast pulse generated is observed at the end of the output line.

The main advantage of this system is to allow the setting of various parameters such as the amplitude, the rise-time or the width of pulses. The pulse width is dependent on the length of the forming line (Figure 29).

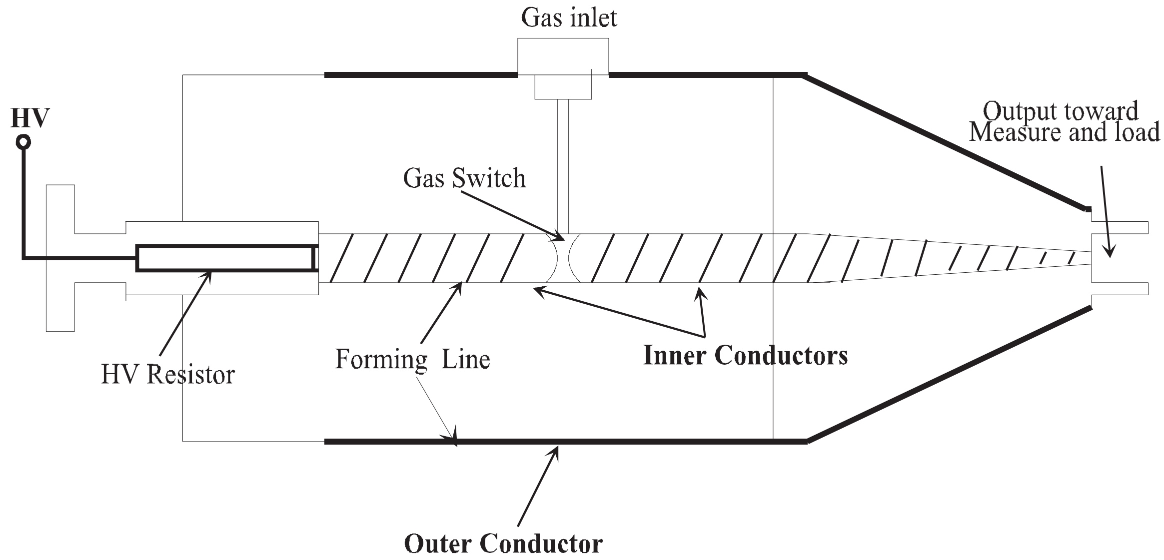

Figure 29. Schematic representation of the coaxial generator using a high pressure gas switch

Different additional forming lines lead to width pulses contained between 600ps and 1.5ns (Figure 30).

Also, the pulse waveform is closely linked to the properties of the switch, and particularly to the gap length, the pressure and the nature of the gas used in the switch filling. The switching element is the major component of any power conditioning system and ultra-fast closing capability. Our technology uses high pressure gas switch in a transmission line structure to produce a powerful UWB pulse. A technical problem concerns the production of the mechanical design. The switch must be able to withstand voltage pulses of 60kV, pressures up to 50bar with no gas leakage and heat from the repetitive spark channel. It is constituted by two brass electrodes terminated with hemispheres made of tungsten.

The switch works on spark discharge. When the gas gap is overvolted, it breaks down and launches a wave between the inner and the outer conductor toward the output end. The dependence on the rise-time with the molecular weight of the filling gas and the electric field

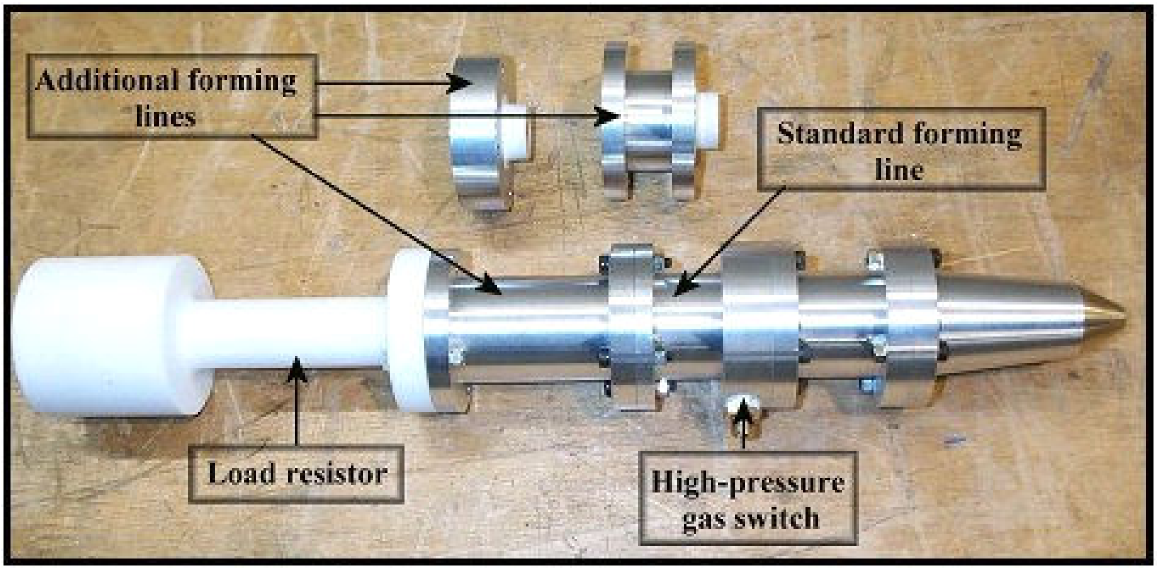

Figure 30. Mechanical machining of the coaxial generator with additional forming lines

into the switch has been shown [24]. That is why hydrogen gas gives the fastest breakdown since it has the lowest density. So, an improvement in recovery time (and thus the PRF) can typically be achieved using hydrogen gas over other atomic gases. The rate of repetitive operation is dependent upon the ability of the HV pulsed source to charge the pulse forming line after each discharge. The pulsed source is used near the top of its possibilities. The pulses generated by this source have 60kV amplitude, 250ns rise-time and the pulse repetition frequency is adjusted to 900Hz. In this case, the pulse repetition frequency is not limited by the recovery time of the gas due to the weak energy of each pulse but by the ability of the pulsed source to load the pulse forming line after each discharge.

Only the pressure of the gas and the gap spacing of the high pressure gas switch varied. The experimental investigations described here were performed on gap spacings of 0.2mm to 0.7mm with the gas pressure being varied between 15bar and 50bar. The amplitude of the output impulse voltage can be adjusted from 3kV to 26kV into a 50Ω impedance. This first test aims at determining associations pressure-gap spacing which allow to vary the pulse amplitude in hydrogen. These results are presented on Figure 31. A linear variation of the pulse amplitude with the product gas pressure time gap spacings is observed in accordance with the right-hand portion of the Paschen curve. So this linear variation seems to consolidate the fact that very fast gas breakdown occurs with classical streamer propagation mechanism leading to breakdown at high pressure. The reproducibility of the results given is relatively good: less than 5% variation when averaged over 30 minutes of functioning at 900Hz.

The rise-time of a gas switch is found to be strongly dependent on the electric field value (Figure 32). Typically, the highest pressure with the shortest gap spacing produces the fastest output rise-times. The rise-time can be controlled continuously by varying the pressure of hydrogen in the switch. Initially it decreases rapidly with increasing applied electric field, then slowly when it saturates at 70ps. A minimum measured rise-time of 70ps (Figure 33) can be obtained thanks to an improvement of the geometry configuration. The rise-time of 70ps is measured with a sampling scope 6GHz bandwidth: the real rise-time is certainly faster because the measurement system leads to an over-evaluation of the rise-time.

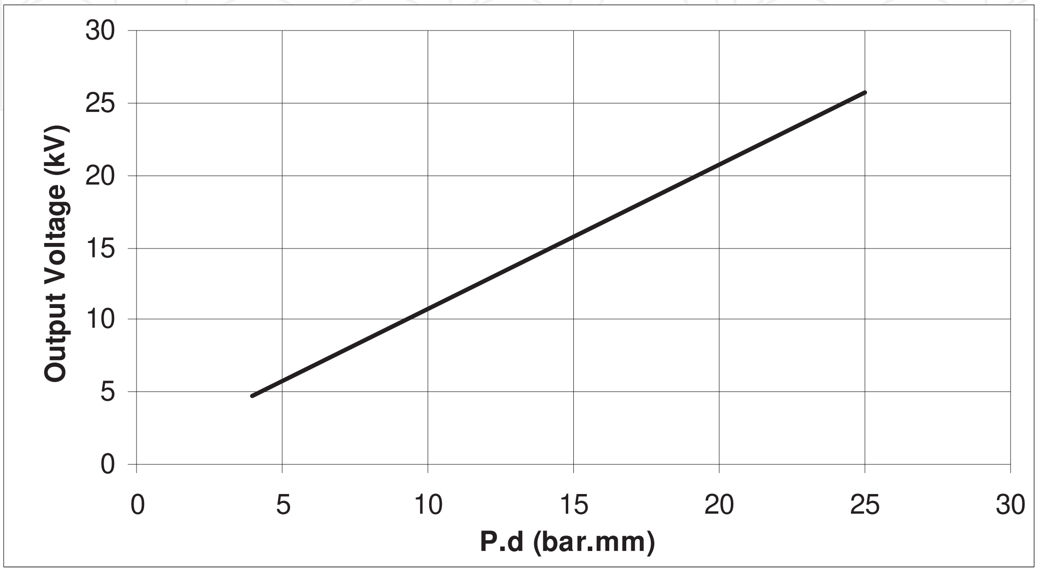

Figure 31. Output voltage versus pressure × gap spacing

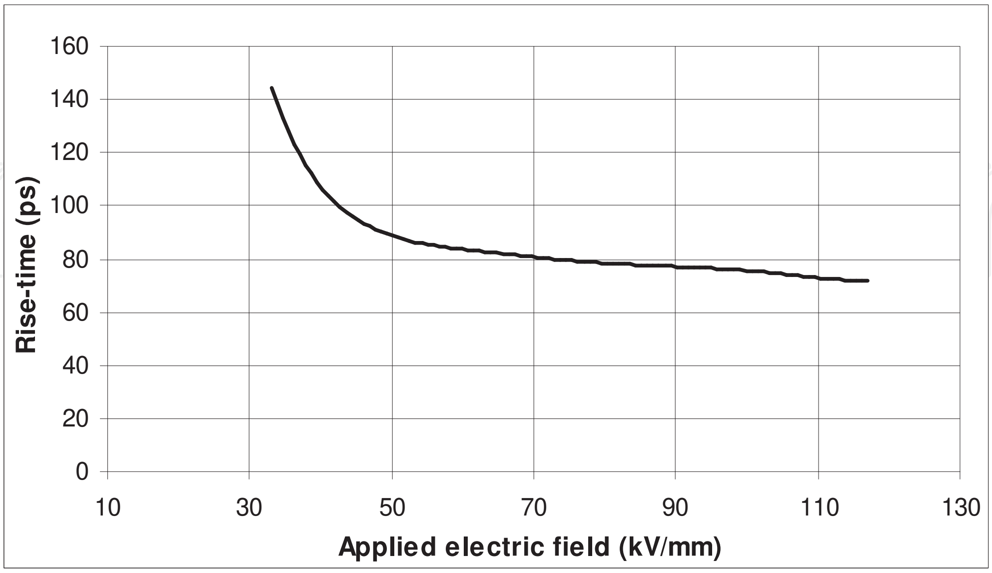

Figure 32. Rise-time of the output pulses versus electric field in the switch

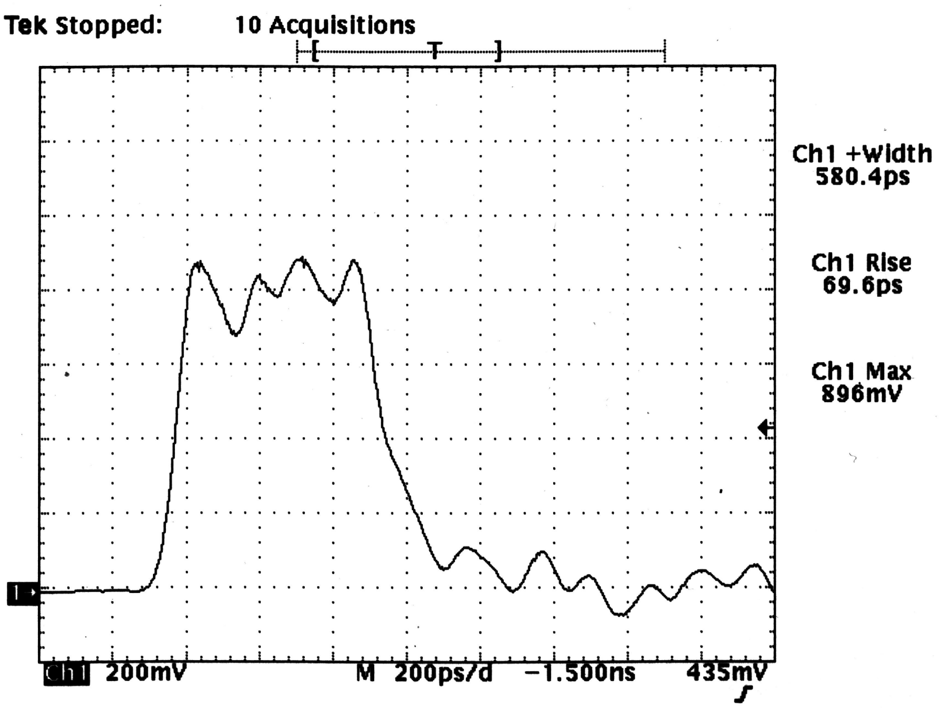

Figure 33. Output pulse shape of the coaxial generator (P=55bar, d=0.45mm, τ=68ps, V_{OUT}=26kV)

4.3. PULSAR: the UWB synthetic aperture radar

The PULSAR radar is dedicated to pulse measurements on outdoor targets and low frequency clutter (Figure 34). This system should allow the detection of landmine under the ground.

The previously described picoseond generator is combined to a radiating structure and they are mounted on a truck. So, the XLIM laboratory (University of Limoges, France) has developed a new radiation device (antenna and balun made by Europulse, France). The antenna, called Dragonfly antenna [25], is able to support high peak voltage (25kV) and has a very large bandwidth (200MHz to 4GHz) as well as a high gain along the axis (up to 12dB). Indeed, the bandwidth of the pulse delivered by the generator must be as wide as possible. Buried mines can thus be detected on all the frequency bands from 200MHz to 4GHz.

To carry out the image processing, it is necessary to eliminate the coupling between antennas and the coupling with the ground by subtraction of the mean transient signal. The aim is to suppress echo interferences to isolate the target response.

The complete generator in association with the Dragonfly antenna and balun was first characterised in an anechoic chamber (Figure 35). The Dragonfly antenna, is made up of four metallic flared plates with a 50Ω input impedance. The input antenna is a symmetrical double-strip transmission line. To build the radiation part of the new antenna, each input strip is divided in two flared plates. The balun ensures the transition between a 50Ω coaxial cable and the 50Ω input impedance fixed by the input planar configuration.

Figure 34. Photographies of the PULSAR UWB synthetic aperture radar

On Figure 36, the measured signal is presented for two Dragonfly antennas facing each other at 10.5 meters (three angles). One of the antennas, connected to our picosecond pulse generator,

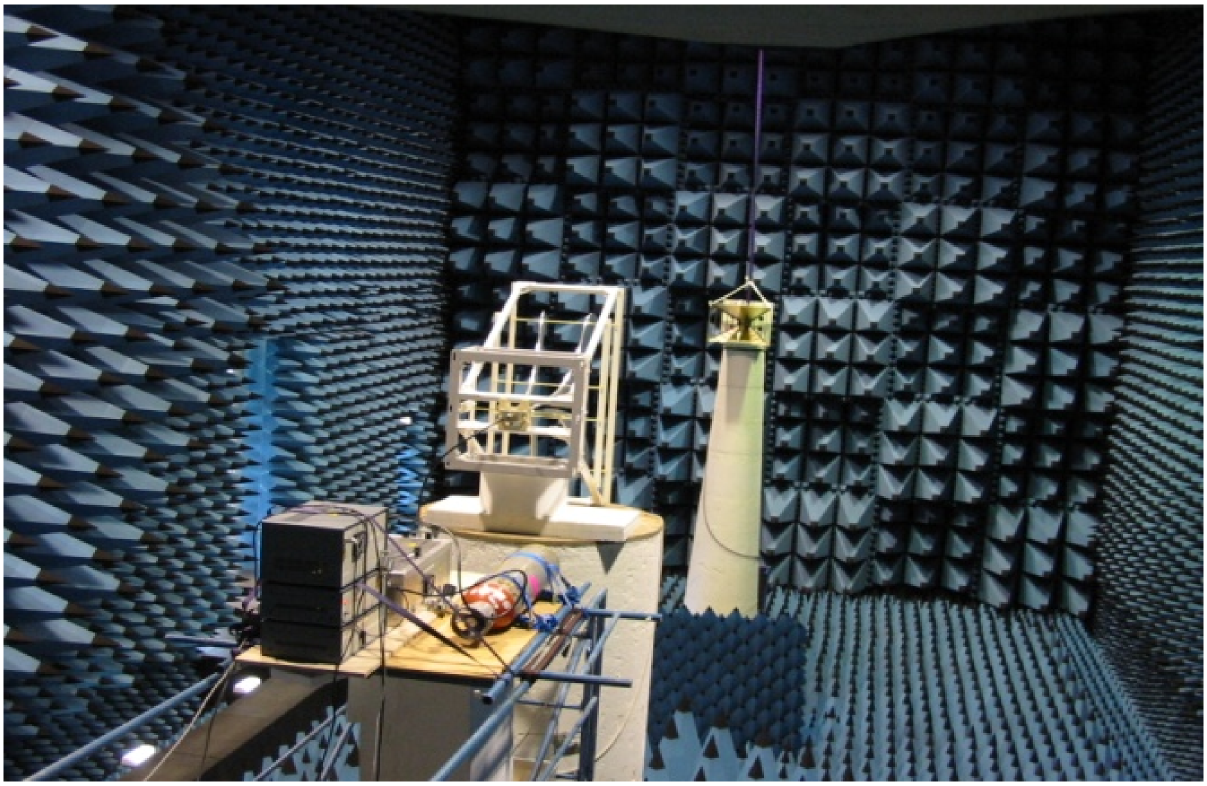

Figure 35. Characterisation test in an anechoic chamber

is used as transmitter. The pulse issued from the pulse generator presents the following characteristics: output voltage 23kV and rise-time of 80ps. The receiving antenna is connected to a digital sampling Tektronix sequential acquisition oscilloscope TDS820 (6GHz bandwidth). The Fourier transform of the measured pulse (Figure 36-b) exhibits a bandwidth from 400MHz to 1.4GHz of -20dB below the maximum.

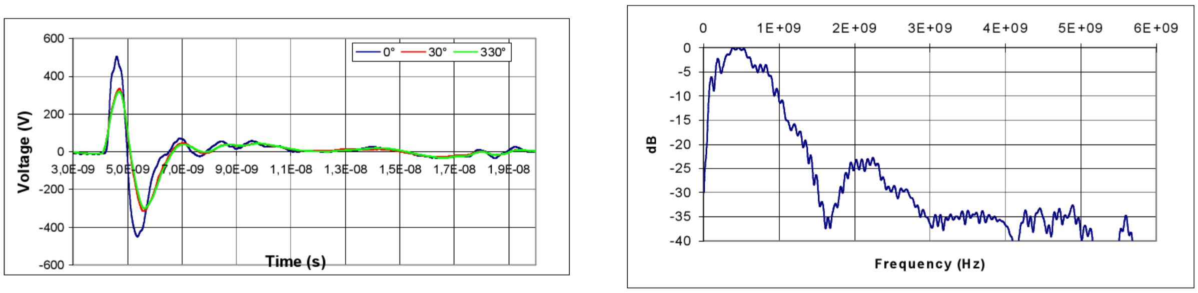

(a) (b)

Figure 36. Measured signal at the receive antenna for antennas positioned facing each other (a) transient response (b) Fourier transform of the transient response

The radiation patterns in H plane and E plane at 500MHz frequency are shown as example in Figure 37. Note that the main lobe is narrower in the H plane than in the E plane and becomes narrower with the frequency increase.

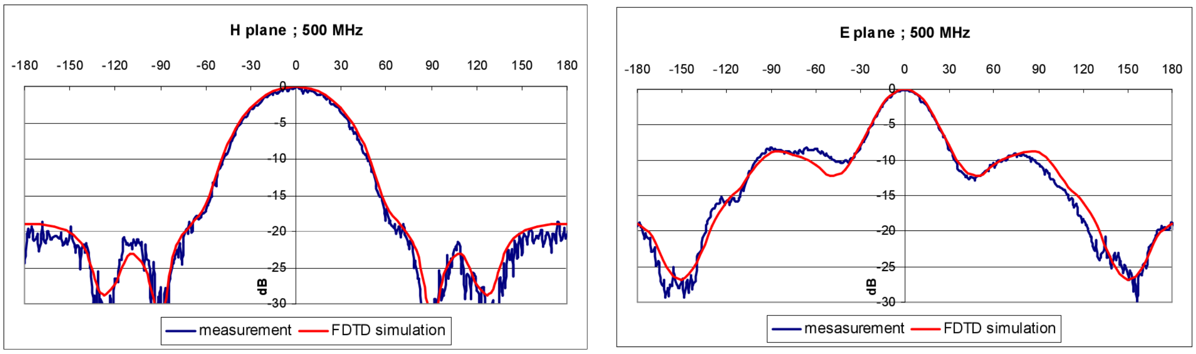

(a) (b)

Figure 37. Radiation patterns in H plane (a) and in E plane (b) (500MHz); transient measurement compared to FDTD method

The bandwidth and field level improve the range and the resolution of the system so that it can detect targets more distant from the emitting antenna. It is now possible to work with the PULSAR system from a height of approximately 10 meters or more [25]. To carry out the image processing, it is necessary to eliminate the coupling between antennas and the coupling with the ground by subtraction of the mean transient signal. The aim is to suppress echo interferences to isolate the target response.

Acknowledgements

These works were sponsored by Thales Communications and by the French Department of Defense (DGA). The authors gratefully acknowledge the CEA (CESTA and GRAMAT), XLIM, CISTEME and TECHNIX for their important contribution to these projects.

Author details

L. Pecastaing[1], M. Rivaletto[1], A. Silvestre de Ferron[1], B. Cadilhon[2] and R. Pecquois[2]

1 Laboratoire SIAME, Université de Pau, Pau, France

2 CEA CESTA, F-33114 Le Barp, France

References

[1] W. J. Carey, A. J. Wiebe, D. D. Schwindt, L. L. Altgilbers, M. Giesselmann, B. McHale, and K. Heinemann, "Autonomous RF Radiation Package for Various Applications," in *2005 IEEE Pulsed Power Conference*, 2005, pp. 218–221.

[2] D. G. Staines and D. J. Urban, "DIEHL High-Power RF Source Development," presented at the EUROEM, Magdeburg, Germany, 2004, pp. 90–91.

[3] R. Stark, "DIEHL HEPM-Source development," presented at the High Power Microwave Defense & Security Workshop, ISL, Saint Louis, France, 2011.

[4] "APELC," *Applied Physical Electronics, L.C.* [Online]. Available: http://www.apelc.com/.

[5] M. G. Mayes, J. R. Mayes, M. B. Lara, and L. L. Altgilbers, "High Voltage Properties of Insulating Materials Measured in the Ultra Wideband," in *2005 IEEE Pulsed Power Conference*, 2005, pp. 954–957.

[6] J. R. Mayes and W. J. Carey, "Compact Pulsed Power Sources," SAE International, Warrendale, PA, SAE Technical Paper 2002-01-3180, Oct. 2002.

[7] J. R. Mayes, M. B. Lara, M. G. Mayes, and C. W. Hatfield, "An Enhanced MV Marx Generator for RF and Flash X-Ray Systems," in *2005 IEEE Pulsed Power Conference*, 2005, pp. 1302–1305.

[8] J. R. Mayes, M. G. Mayes, W. C. Nunnally, and C. W. Hatfield, "Helical antennas for high powered RF," in 2009 *IEEE Pulsed Power Conference*, 2009, pp. 484–488.

[9] K. D. Hong and S. W. Braidwood, "Resonant antenna-source system for generation of high-power wideband pulses," *IEEE Transactions on Plasma Science*, vol. 30, no. 5, pp. 1705–1711, Oct. 2002.

[10] K. Hong and S. Braidwood, "Development of antenna-source system for generation of high-power electromagnetic pulses," in *Pulsed Power Plasma Science, 2001. PPPS-2001. Digest of Technical Papers*, 2001, vol. 1, pp. 203–206 vol.1.

[11] P. Sarkar, S. W. Braidwood, I. R. Smith, B. M. Novac, R. A. Miller, and R. M. Craven, "A Compact Battery-Powered 500kV Pulse Generator for UWB Radiation," in *2005 IEEE Pulsed Power Conference*, 2005, pp. 1306–1309.

[12] P. Sarkar, S. W. Braidwood, I. Smith, B. M. Novac, R.. Miller, and R. M. Craven, "A Compact Battery-Powered Half-Megavolt Transformer System for EMP Generation," *IEEE Transactions on Plasma Science*, vol. 34, no. 5, pp. 1832–1837, Oct. 2006.

[13] D. V. Giri, F. M. Tesche, M. D. Abdalla, M. C. Skipper, and M. Nyffeler, "Switched Oscillators and Their Integration Into Helical Antennas," *IEEE Transactions on Plasma Science*, vol. 38, no. 6, pp. 1411–1426, 2010.

[14] J.D. Taylor, "Introduction to Ultra wideband radar systems", Ed WC Nunally et al (Boca raton, FL: CRC Press), ch. 6, p 287, 1995.

[15] L. Pecastaing, T. Reess, J. Paillol, A. Gibert, P. Domens, "Very fast rise time short pulse high voltage generator", *IEEE Transactions on Plasma Science*, vol. 34, N°5, Part 1, pp. 1822-1831, 2006.

[16] J.C. Diot, P. Delmote, J. Andrieu, M. Lalande, V. Bertrand, B. Jecko, S. Colson, R. Guillerey, M. Brishoual, "A novel antenna for transient applications in the frequency band 300MHz-3GHz: the "Valentine" antenna", *IEEE Transactions on Antennas and Propagation*, vol. 55, n°3, pp 987-990, 2007.

[17] P. R. Foster, S. M. Tun, "A wideband balun from coaxial line to TEM line", In Proc. of the *IEE Conference on Antennas and Propagation*, pp. 286-290, 1995.

[18] E. G. Farr, G. D. Sower, C. J. Buchenauer, "Design Considerations for Ultra-Wideband, High-Voltage Baluns", *Sensor and Simulation Notes*, n°371, 1994.

[19] B. Cadilhon, "Study and realisation of an autonomous source of high-power electromagnetic waves", Ph. D dissertation, n° 08PAUU3008, Pau University, France, 2008.

[20] S. Vauchamp, J.C. Diot, M. Lalande, J. Andrieu, B. Beillard, B. Jecko, J.L. Lasserre, A. Paupert, G. Teyssidou, R. Pouzalgues, "Utilization of a target diffraction to measure a high electromagnetic field", In *International Conference on Electromagnetics in Advanced Applications*, pp 784-787, Sept. 2007

[21] S. Vauchamp, M. Lalande, J. Andrieu, B. Jecko, J.L. Lasserre, L. Pecastaing, B. Cadilhon, "Utilization of target scattering to measure high level electromagnetic fields: the MICHELSON method, IEEE Instrumentation and Measurement, Volume 59, Issue 9, pp 2405-2413, 2010

[22] B. Cadilhon, L. Pecastaing, T. Reess, A. Gibert, "Low stray inductance structure to improve the rise-time of a Marx generator", *IET Electric Power Applications*, Volume 2 Issue 4, pp. 248-255, 2008

[23] B. Cadilhon, B. Cassany, J-C. Diot, P. Modin, E. Merle, L. Pecastaing, A. Silvestre de Ferron, M. Rivaletto, V. Bertrand, "Self-contained, hand portable and repetitive ultra-wideband radiation source", *IEEE Transactions on Plasma Science*, Volume 6, Part 2, pp 1549-1559, 2011

[24] L. Pecastaing, J. Paillol, T. Reess, A. Gibert, P. Domens, "Design and performance of high voltage pulse generators for ultra-wideband applications", *Measurement Science and Technology*, vol 12, pp. 1718-1725, 2001

[25] P. Delmote, C. Dubois, J. Andrieu, B. Beillard, M. Lalande, V. Bertrand, B. Jecko, L. Pecastaing, A. Gibert, J. Paillol, P. Domens, R. Guillerey, F. Monnier, M. Legoff, "The UWB SAR system PULSAR : new generator and antenna developments", In *SPIE International Conf*erence, AeroSense, Orlando, 2003